

Review article

Advanced biological and non-biological technologies for carbon sequestration, wastewater treatment, and concurrent valuable recovery: A review

Santosh Kumar^a, Monali Priyadarshini^b, Azhan Ahmad^c, Makarand M. Ghangrekar^{a,b,c,*}

^a PK Sinha Centre for Bioenergy and Renewables, Indian Institute of Technology Kharagpur, Kharagpur 721302, India

^b School of Environmental Science and Engineering, Indian Institute of Technology Kharagpur, Kharagpur 721302, India

^c Department of Civil Engineering, Indian Institute of Technology Kharagpur, Kharagpur 721302, India

ARTICLE INFO

Keywords:

Carbon sequestration
Electrochemical reduction
Greenhouse gas
Microbial electrochemical technologies
Photocatalyst

ABSTRACT

Over the last few years, mitigation of global warming has become a challenge for researchers. Therefore, CO₂ conversion into energy-rich valuables and fuels can become a crucial strategy for abating the growing global CO₂ emission. However, the CO₂ molecule is highly stable, which requires large over potential for converting it to valuable chemicals; thus, making its reduction quite difficult. In this regard, technologies, such as microbial electrochemical technology (MET), photocatalytic and electrochemical technologies triggered considerable interest in the reduction of CO₂. These technologies can help in solving the global climate issue based on mitigating the CO₂ into the desired product like formic acid, methanol, methane, and other valuables with low energy consumption and minimal carbon emission. Thus, the objective of this review is to provide an updated critical discussion on the recent progress in application of biological and non-biological technologies for CO₂ reduction and wastewater treatment. Moreover, the mechanism governing the microbial, photocatalytic, and electrocatalytic CO₂ reduction and pollutant removal from wastewater along with a detailed discussion of catalysts used in these technologies are also highlighted. Further, brief prospective and future recommendations on the development of efficient CO₂ reduction technologies have also been elucidated in this article, which could be vital for enhancing the conversion efficiency of CO₂ in the reduction system.

1. Introduction

Recently, with the furtherance of society and industrial development, worldwide energy consumption is increasing swiftly and it is predicted to rise about 28 %, from 6.067×10^{20} Joule in 2015 to about 7.765×10^{20} Joule in 2040 [1]. Despite the recent efforts by researchers to expand carbon-neutral energy sources, fossil fuels based on

non-renewable energy sources are still speculated to remain the major root for fulfilling energy demand in the near future. However, fossil fuel use to meet energy demand can give rise to global greenhouse gas (GHG) emissions, such as CO₂ and CH₄ that impact to global climate change and emission of other polluting gasses, such as NO_x and SO_x. For example, per year global CO₂ emission has risen to about 30–40 gigatonnes and it is estimated to continue increasing in coming years owing to

Abbreviations: BES, Bio-electrochemical system; CB, Conduction band; CCM, Carbon concentration mechanism; CF, Carbon felt; CNFs, Carbon nanofibers; CNTs, Carbon nanotubes; CNG, Compressed natural gas; COD, Chemical oxygen demand; DCMFC, Double chamber microbial fuel cell; DERC, Direct electrochemical reduction of gaseous CO₂; DET, Direct electron transfer; DO, Dissolved oxygen; EMIM, 1-ethyl-3-methylimidazolium; ENMs, Engineered nanomaterials; ESR, Electron spin resonance; ET, Electron transfer; GHG, Greenhouse gas; GQDs, Graphene quantum dots; HER, Hydrogen evolution reaction; IoT-WSN, Internet of Things-based wireless sensor network; MCC, Microbial carbon-capture cell; MEC, Microbial electrolysis cells; MECC, Microbial electrolytic carbon capture; MES, Microbial electrosynthesis; MOFs, Metal-Organic Frameworks; METs, Microbial electrochemical technology; MREC, Microbial reverse-electrodialysis electrosynthesis cell; ORR, Oxygen reduction reaction; PEDOT, Poly 3,4-ethylene dithiophene; PEM, Proton exchange membrane; P-MFC, Plant-microbial fuel cell; QDs, Quantum dots; SHE, Standard hydrogen electrode; SMFC, Submerged macrophyte sediment microbial fuel cell; TEM, Transmission electron microscopy; TOC, Total organic carbon; TRF, Time-resolved fluorescence; TRL, Technology readiness level; TSS, Total suspended solids; UV, Ultraviolet; VB, Valance band; VFA, Volatile fatty acid; WWTP, Wastewater treatment plant; WW, Wastewater; XAS, X-ray absorption spectroscopy.

* Corresponding author at: PK Sinha Centre for Bioenergy and Renewables, Indian Institute of Technology Kharagpur, Kharagpur 721302, India.

E-mail address: ghangrekar@civil.iitkgp.ac.in (M.M. Ghangrekar).

<https://doi.org/10.1016/j.jcou.2022.102372>

Received 13 October 2022; Received in revised form 9 December 2022; Accepted 12 December 2022

Available online 19 December 2022

2212-9820/© 2022 The Authors. Published by Elsevier Ltd. This is an open access article under the CC BY license (<http://creativecommons.org/licenses/by/4.0/>).

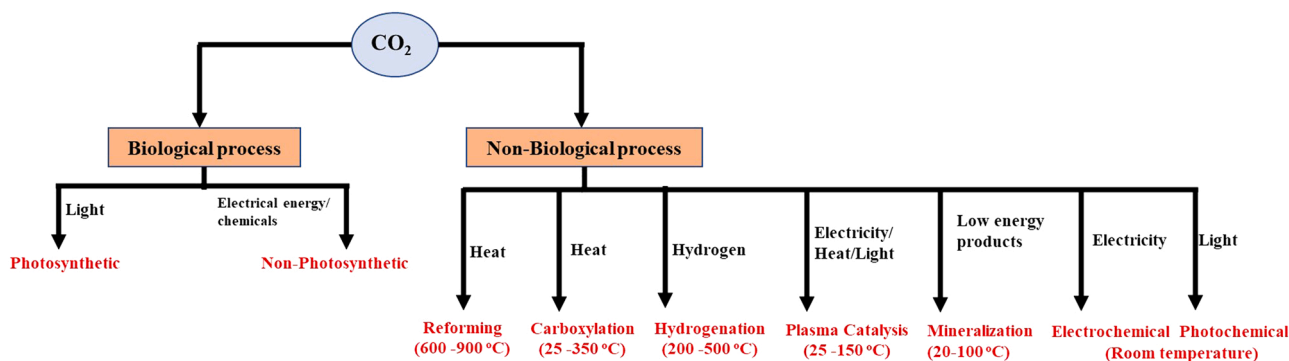


Fig. 1. Biological and non-biological CO₂ reduction technologies.

urbanization and industrialization [2]. Hence, reducing CO₂ to chemical fuels is a critical issue for the global scientific society to attain the carbon-neutral energy requirement and mitigate the climate change challenges.

Research has been focused in the recent past on reducing CO₂ into value-added products, and advanced biological and non-biological treatment technologies, including electrochemical and photochemical, are utilized for CO₂ reduction along with the degradation of organic pollutants. For instance, in the case of biological treatment, microbial electrochemical technology (MET) such as microbial electrosynthesis (MES), microbial carbon-capture cell (MCC), microbial electrolytic carbon capture (MECC), and plant-microbial fuel cell (P-MFC) are potential technologies used for CO₂ capture with concurrent contaminated water treatment, as well as recovery of valuables. In MES, CO₂ is used as a substrate that is reduced to produce multi-carbon organic compounds in the presence of biocatalysts. However, P-MFC uses atmospheric CO₂ during photosynthesis as well as consumes nitrates, phosphate, and other contaminants present in the wastewater as substrate for plant growth, offering effective wastewater treatment. The microalgae-bacteria consortium can be used in mitigating CO₂ and utilizing it as carbon source for the growth of algae and bacteria [3]. Moreover, based on several investigations, the microalgae have about 10–50 folds more CO₂ fixation rate as compared to terrestrial plants [4]. Thus, making algal-based biological treatment a potential technology for mitigating possible global warming changes.

On the other hand, electrochemical and photoelectrochemical technologies require a catalyst to promote a CO₂ reduction reaction. Since the final carbon product (CO₂) is thermodynamically a very stable molecule; thus, elevated activation energy is required for reducing CO₂ to CO₂ ($E^\circ = -1.90$ V Vs SHE at pH = 7.0) [5]. Moreover, CO₂ reduction also engage with the hydrogen evolution reaction (HER), a cathodic half-reaction occurring at the lower overpotential ($E^\circ = 0$ V Vs SHE at pH = 7.0) [5]. This side reaction needs to be overcome to achieve CO₂ reduction; thus, an ideal electro catalyst is required, which can diminish the activation barrier of the CO₂ reduction reaction as compared to HER [6]. Hence, CO₂ reduction can be obtained with higher reaction rates even at low overpotential.

The electrocatalyst for CO₂ reduction is majorly categorized as metallic and non-metallic catalyst. Based on the formation of reduction product the metallic catalyst can be CO selective catalyst (Au, Zn, and Ag), formate selective catalyst (Sn, Pb, and In) and hydrogen selective catalyst (Fe, Pt, and Ni) [7]. However, among the metallic catalyst Cu shows a distinct catalytic activity to produce a wide variety of CO₂ reduction products like formate, ethylene, ethanol, and CO [8]. Similarly, a carbon-based composite catalyst, such as carbon-doped molybdenum sulphate was also utilized as a CO₂ reduction catalyst in electrochemical and photo-electrochemical technologies [9].

Until September 2022, according to a bibliographic search in the Scopus database using the keywords “photocatalytic CO₂ sequestration” and “photocatalytic CO₂ reduction,” about 4942 articles were available

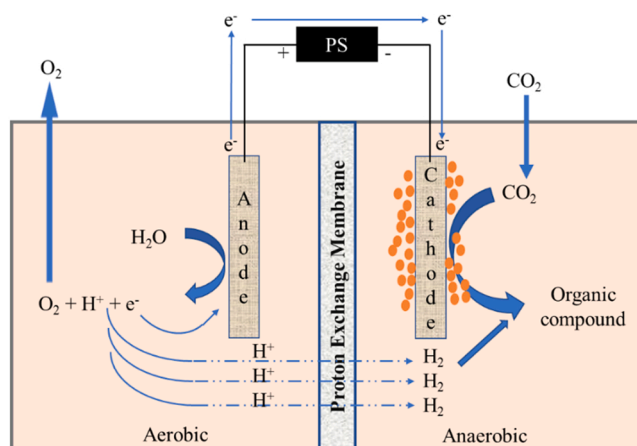


Fig. 2. Schematic of a typical microbial electrosynthesis setup.

for the photocatalytic CO₂ sequestration. Similarly, for the MET system a total of 71 articles were available with the keywords “microbial electrochemical technology CO₂ sequestration” and “microbial electrochemical technology CO₂ reduction”. For electrocatalytic CO₂ reduction, 2952 articles were available with the keywords “electrocatalytic CO₂ reduction” and “electrocatalytic CO₂ sequestration”. The available articles lack complete comparative reviews of innovative biological and non-biological CO₂ capture. This present review article elucidates the comparative CO₂ capturing efficiency of different technologies, such as MET, electrocatalytic and photocatalytic systems. To the best of our knowledge, no such review is available in the literature that juxtaposes these state-of-the-art technologies for assessing their efficacy in sustainable CO₂ capturing. A comparison of these technologies in terms of mechanism, application, and operation has been discussed here. Additionally, benefits and applications of hybrid systems for CO₂ reduction are also elucidated. Moreover, this article also highlights the efficiency of wastewater treatment and value-added product recovery with these systems.

2. CO₂ reduction technologies

The CO₂ reduction technologies are categorized into biological and non-biological transformations according to the mode of use of energy sources (Fig. 1). However, the basic insight of MET for CO₂ reduction and comparison with other CO₂ transformation technologies have not been clearly documented to date. Thus, this present review discusses the fundamentals, mechanisms, advantages, and disadvantages of recently reported METs for CO₂ conversion. Moreover, a comparison in terms of cost analysis and maturity of electrochemical, photochemical, and biological processes has also been elucidated in the following sections.

2.1. Biological processes

2.1.1. Microbial electrosynthesis

The MES is an emerging technology, which is capable of CO₂ capture, wastewater treatment, and simultaneously electro-fuels can be produced via microbial metabolism [10]. A typical MES consists of a biotic cathodic chamber, an abiotic anodic chamber, and a proton exchange membrane (PEM) that separates the anodic and cathodic chambers (Fig. 2). In the anodic chamber, electrochemical water splitting takes place using external potentiostat to produce protons (H⁺), electrons (e⁻), and oxygen (O₂). The e⁻ migrates from anode to cathode through the conductive wire by the action of the external potentiostat. The H⁺ produced are transferred from the anodic chamber to the cathodic chamber through PEM [11]. The CO₂ is a substrate for anaerobic microbes in the cathodic chamber to produce value-added products, such as acetic acids and methane [12].

The performance of a MES depends on various factors, such as microbial inoculum, reactor configuration, wastewater quality, ambient temperature, potential applied, etc.; however, selecting electrode material is one of the major components. The MES necessitates biocompatible electrode materials with a large specific surface area, supporting biofilm development for elevated current densities to offer significant product yield [13]. The common electrode materials used in MES are carbonaceous materials (biochar, activated carbon, carbon nitride, carbon nanotubes, graphene, reticulated vitreous carbon, and carbon cloth/brush/rod), metallic materials (metal oxide, stainless steel, and metals like Fe, Pt, Pd, Au, Mo, Ni, etc.), and carbon-metallic materials (metal and metal oxides coated with carbonaceous materials, and carbonaceous materials coated with metals or metal oxide) [14]. However, biocompatible carbon-metallic materials are relatively more advantageous in terms of good catalytic effect and harvesting high power density [15].

According to a recent investigation, the acetate production rate in CuO/g-C₃N₄ photocathode-based MES was 0.16 g L⁻¹ d⁻¹, which is 2.6 times higher than that of control MES (0.06 g L⁻¹ d⁻¹) [16]. In another investigation, the acetate production rates in MES with TiO₂ (2.15 g L⁻¹ d⁻¹) and Rh (1.06 g L⁻¹ d⁻¹) cathode were 2.14 and 1.3 times higher compared to control (0.82 g L⁻¹ d⁻¹) operated without any catalyst [17]. Similarly, an investigation of CH₄ production in MES with magnetic assembling GO/Fe₃O₄/microbes as hybridized biofilms on carbon cloth resulted in the yield of 605 ± 119 mmol m⁻² d⁻¹, which is a 14.5-fold increase compared to a control MES with carbon cloth biofilm that produces 42 ± 7 mmol m⁻² d⁻¹ [18].

2.1.1.1. Application of MES

2.1.1.1.1. CO₂ capture and value-added chemical production. The MES is the leading CO₂ capture bio-electrochemical system (BES) that converts CO₂ into valuable products, such as acetate, methane, and short-chain fatty acids [19]. The electroactive microbes are the core components of MES that consumes atmospheric CO₂ as the main carbon source. The sustainability or efficiency of this system depends on the metabolic properties and e⁻ uptake ability of these electroactive microbes. These microbes are mostly chemoautotrophic bacteria (nitrogen-fixing bacteria, sulphur-oxidizing bacteria, and iron-oxidizing bacteria) and can take e⁻ directly from electrodes; however, to accelerate the interfacial e⁻ transfer from electrodes to microbes, electrically active redox mediators, such as 4-naphthoquinone, hydroquinone, 2-hydroxy-1, etc., were used in the previous investigations [20].

The products formed from the bio-electrochemical transformation of CO₂ depend on the dominance of bacterial species existing in the cathodic chamber of MES [21]. In the case of mixed anaerobic culture in the cathodic chamber, acetogens and methanogens are generally dominant in producing acetate and methane; however, other organic compounds can be obtained by manipulating the operational parameters [12]. In practice, both mixed as well as pure microbial cultures are

Table 1

Value-added products and biochemical reaction at anode and cathode of MES.

Value-added products	Anode reaction	Cathode reaction
Acetic acid	$C_xH_yO_z \rightarrow CO_2 + H^+ + e^-$	$2CO_2 + 8H^+ + 8e^- \rightarrow CH_3COOH + 2H_2O$
CH ₄	$C_xH_yO_z \rightarrow CO_2 + H^+ + e^-$	$CO_2 + 8H^+ + 8e^- \rightarrow CH_4 + 2H_2O$
Formic acid	$C_xH_yO_z \rightarrow CO_2 + H^+ + e^-$	$CO_2 + 2H^+ + 2e^- \rightarrow HCOOH$
H ₂	$C_xH_yO_z \rightarrow CO_2 + H^+ + e^-$	$2H^+ + 2e^- \rightarrow H_2$
Butyric acid	$C_xH_yO_z \rightarrow CO_2 + H^+ + e^-$	$4CO_2 + 20H^+ + 20e^- \rightarrow CH_3CH_2CH_2COOH + 6H_2O$
Ethanol	$C_6H_{12}O_6 \rightarrow 2CH_3CH_2OH + 2CO_2$	$2CH_3COOH + 4H^+ + 4e^- \rightarrow CH_3CH_2OH + 3H_2O$

implemented in MES. However, a mixed culture is more feasible for field-scale MES owing to high tolerant to various environmental changes [22]. Different biochemical reactions for the synthesis of value-added products in MES are summarized in Table 1.

Electrosynthesis systems are generally operated at higher temperatures as an increase in temperature up to 100 °C increases the electrochemical conductivity of heterogeneous catalysts (according to the Arrhenius relationship) [23]. The lower yield challenges of MES can be resolved by operating it at a higher temperature; however, organics formation in MES is mostly demonstrated by the metabolic activity of mesophilic bacteria within a temperature range of 15–45 °C [24]. In this regard, applying thermophilic bacteria in MES could increase the system's efficiency as operation under thermophilic conditions (> 45 °C) will increase the substrate solubility, mass transfer rate, and microbial activity as well as lower the risk of contaminations. According to Yu et al. the rates of microbial electrosynthesis of formate and acetate at 50 °C using *Moorella thermoautotrophica* were 23.2 and 2.8-fold more than at 25 °C, respectively [25]. In another investigation, when anaerobic sludge (mesophilic) was used in a lab-scale MES at 50 °C to develop a resilient biocathode, a higher amount of acetate (5250 mg L⁻¹) was obtained during a prolonged operational period of 150 days with a maximum production rate of 28 g m⁻² d⁻¹ [26].

Value-added product recovery in MES utilizing CO₂ is highly desirable; however, the specific operational parameters are the key for synthesizing desired products. In this regard, in an investigation of the continuous conversion of CO₂ to methane, acetate, and ethanol in MES, the methane production rate of 1.3 L(L_{RD})⁻¹ was reported below the cathode liquid pH value of 8.0 at a CE of 90–94 %; however, the formation of acetate predominated above pH of 8.5 [27]. Furthermore, continuous operation of the MES at high cathodic pH led to the formation of ethanol; after 80 days of operation, the acetate and ethanol concentrations of 5 g L⁻¹ and 8 g L⁻¹, respectively, were reported in the effluent with a CE of above 80 % [27]. Again, according to Li et al. in a microbial reverse-electrodialysis electrosynthesis cell (MREC), the CO₂ conversion to ethanol and acetate a production rate of 130.75 ± 8.75 and 137.92 ± 7.92 mmol m⁻² d⁻¹, respectively, was reported with low-grade waste heat energy coupled with thermolytic solutions (NH₄HCO₃ solution) [28]. Similarly, other investigations have also adapted MES to transform CO₂ into valuable products as summarized in Table 2.

2.1.2. Plant microbial fuel cell

Plant microbial fuel cell (P-MFC) has emerged as an innovative, promising, and environmentally friendly system for the generation of bioenergy along with synchronized wastewater treatment, valuable product recovery, and CO₂ sequestration [35]. In P-MFC, cultivating plant in the anodic chamber was implemented to provide organic material as a substrate for the bacteria (rhizobium) present at the root nodules of plants [36]. Moreover, plants get the nutrients for their growth from wastewater, which is at the same time treated in the anodic chamber of the P-MFC. During photosynthesis process, these plants

Table 2
Value-added products recovery from MES.

Product	Wastewater/waste	Inoculum	Cathode	Working potential (V vs. Ag/AgCl)	Rate of production	Reference
Acetate	DSMZ 311 media	<i>S. ovata</i>	Synthetic biofilm onto a carbon cloth cathode	−0.8	0.31 g L ^{−1} d ^{−1}	[29]
Acetate	Synthetic bacterial media	Mixed culture from the effluent of an anaerobic digester	CF	−1.11	0.276 – 0.44 g L ^{−1} d ^{−1}	[30]
Acetate	Synthetic catholyte	Mixed culture	Stainless steel mesh with PU particles	−1.27 (vs. SHE)	1.65 g L ^{−1} d ^{−1}	[31]
Acetate	Synthetic catholyte	Mixed culture from anaerobic Sewage Treatment Plant	Graphite plates	−0.995 (vs. SHE)	~ 35.65 mg L ^{−1} d ^{−1}	[32]
Acetate	Synthetic nutrient solution	Mixed culture WWTP sludge	CF	−0.9	42.2 mg L ^{−1} d ^{−1}	[33]
CH ₄	Synthetic catholyte	MEC effluent	Magnetic assembling GO/Fe ₃ O ₄ /Microbes as hybridized biofilm	−0.9	0.6049 mol m ^{−2} d ^{−1}	[18]
CH ₄	Synthetic catholyte	Effluent of a CH ₄ -producing MES	Stainless steel/graphene foam	−1	0.848 mol m ^{−2} d ^{−1}	[34]

Note: CF-carbon felt; MEC-microbial electrolysis cells

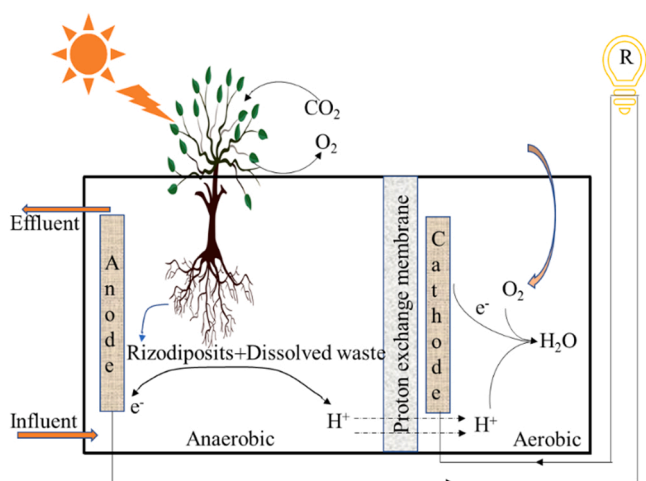
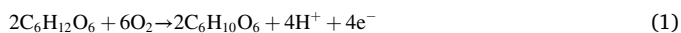


Fig. 3. Schematic representation of the working of a plant-microbial fuel cell.

absorb water from roots, sunlight and CO₂ from the atmosphere and release rhizodeposits (carbohydrates, organic acid, enzymes, sugar, and dead-cell plant material) into the soil or water in the form of root exudates (Fig. 3). On the other hand, the electrogenic bacteria naturally present in the anodic chamber around the plant's roots oxidize the dissolved organics and rhizodeposits, releasing e[−] and H⁺ in the process [37]. The e[−] reduced the anode that is placed close to the plant roots, and H⁺ migrates through the PEM from the anodic to the cathodic chamber, which generates a potential difference across the two chambers; hence, electricity production from solar energy takes place. Also, the H⁺ through PEM and e[−] at the cathode surface combine with free O₂ (as a terminal electron acceptor) to produce water [37,38].

The overall bio-electrochemical reactions taking place in the anodic and cathodic chambers of the P-MFC are shown in Eq. (1) and Eq. (2), respectively [39].



2.1.2.1. Applications of P-MFC. The primary purpose of using a P-MFC is to produce surplus organic matter (rhizodeposits) in the rhizosphere for electrogenic microorganisms to generate reliable bio-electricity. However, P-MFC has many innovative applications, such as wastewater treatment, CO₂ capture, heavy metal removal from a contaminated environment, soil remediation, biosensors, and plant disease

management. A few essential applications of P-MFC are discussed in this section.

2.1.2.1.1. Wastewater treatment. The P-MFC contributes to the removal of organic and inorganic pollutants from wastewater. However, efficiency and sustainability of the system depend on various physico-chemical parameters and the photosynthetic plants used for the treatment process. Some of the critical applications of P-MFC as wastewater treatments are decolorization of an azo dye, antibiotic removal, degradation of nitrobenzene, and other emerging contaminants removal [39].

In this regard, Venkata Mohan et al. obtained chemical oxygen demand (COD) and volatile fatty acid (VFA) removal of 1170 mg L^{−1} (86.67 %) and 418 mg L^{−1} (72.32 %), respectively, using P-MFC with power generation of 224.93 mA m^{−2} after 125 days of operation [40]. Similarly, in a recent investigation on wastewater treatment through a hybrid constructed wetlands and MFC with influent COD and NH₄Cl concentrations of 222 mg L^{−1} and 20 mg L^{−1}, respectively, the maximum COD and NH₄⁺-N removal efficiencies of 86.28 % and 96.82 % were obtained [41]. The efficiency of P-MFC also depends on the type of plant used due to differences in their metabolism and growth rate. In this regard, submerged macrophyte sediment microbial fuel cell (SMFC) using *Ceratophyllum demersum* L., *Vallisneria spiralis* L., and *Hydrilla verticillata* were operated. The *Ceratophyllum demersum* L. based SMFC stood out with maximum power and pollutant removal. The COD removal and power density were 81.16 % and 24.56 mW m^{−2} in this investigation, respectively [42]. In another study of SMFC use of different plants, such as: *Schoenoplectus triquetus*, *Typha latifolia*, *Phragmites australis*, *Juncus*, and *Cyperus alternifolius*, was investigated. The maximum COD reduction values for *S. triquetus*, *T. latifolia*, *P. australis*, *Juncus*, and *C. alternifolius* were 91.4 %, 90.4 %, 86.6 %, 73.3 %, and 72.3 %, respectively, while the total suspended solids (TSS) removal values were 86 %, 80 %, 79.6 %, 78.4 %, and 64 %, respectively [43]. Thus, applying P-MFC for wastewater treatment with simultaneous CO₂ capture and power recovery can be a potential futuristic solution.

2.1.2.1.2. CO₂ capture. The P-MFC might be one of the potential partial contributors to reduce the CO₂ level in the atmosphere. The biochemical pathways for CO₂ capture are the same for all plants; moreover, the CO₂ capture rate is more for fast-growing plants (such as bamboo) [38]. *Azolla* is a fast-growing aquatic plant with a doubling time of 2–5 days under optimum growing conditions. An annual CO₂ capture of about 21,000 kg per year was estimated per hectare of *Azolla* cultivation in a pond [44]. In another demonstration, to improve the power generation of paddy plants in P-MFC, *Azolla* was cultivated, which helps in enhancing three times more power generation (22 mW m^{−2}) compared to only paddy plant P-MFC (3.3 mW m^{−2}) [45]. This investigation revealed the symbiotic application of different plant species to improve the efficiency of P-MFC for CO₂ sequestration,

Table 3

Power generated in P-MFC using different plant species.

Plant species	Substrate	Electrode	Operational period (days)	Power generation (mW m^{-2})	Reference
<i>Oryza sativa</i>	Paddy Field (type 1)	Graphite felt	70	9.1	[54]
	Paddy Field (type 2)			16.8	
<i>Oryza sativa</i> L.	A mixture of potting mix and sandy loam soil in the volume ratio of 3:7, respectively	Carbon felt	125	41.41	[55]
<i>Glyceria maxima</i>	Fed with the adapted ammonium rich 1/2 Hoagland solution	Graphite felt	85	10	[56]
		Graphite granules		12	
<i>Epipremnum aureum</i>	Garden soil and Cow dung of IIT Guwahati campus in the ratio of 3:2, respectively	Acid-treated carbon fiber brush electrode	60	15.38	[57]
<i>Scirpus Validus</i>	Wastewater containing Cr (VI)	Two layers of carbon felt sandwiched between stainless steel wire mesh	–	40.6	[58]

power generation, and nutrient removal. Anthropogenic CO₂ and wastewater from large-scale stationary sources like power plants and refineries are extra burdens that tremendously reduce the quality of the atmosphere and natural water bodies. Thus, implementation of large-scale P-MFC at the source station will not only result in CO₂ capture; however, it will result in wastewater treatment and a surplus bio-electricity generation.

2.1.2.1.3. Bio-electricity generation. A P-MFC is a derivative of MFC, wherein plant roots directly excrete rhizodeposits to fuel the electrochemically active bacteria in the anodic chamber to generate bio-electricity. The P-MFC is a comparatively sustainable technology as it can produce 18 times more power than traditional SMFC [46]. The increased power generation can be explained by the availability of rhizodeposits for microbial oxidation. Research has been performed on evaluating performance of P-MFC under different operational conditions, as summarized in Table 3. In an investigation of steam-coupled PMFCs using *Populus alba* and *Pachira macrocarpa*, the output power densities of 7.61 mW m^{-2} and 3.60 mW m^{-2} , respectively, were obtained [47]. In another investigation of P-MFC, when the power output of the plant species is compared, the *Wachendorfia thyrsiflora* produced the highest ($1036 \pm 59 \text{ mW m}^{-3}$) followed by *Cyperus papyrus* ($510 \pm 92 \text{ mW m}^{-3}$); whereas the lowest power output was measured in control (no plant, $392 \pm 67 \text{ mW m}^{-3}$) [48].

The application of P-MFC for bioelectricity recovery with simultaneous food crop yield was investigated using *Amaranthus viridis* and *Triticum aestivum* cultivation with and without bio-slurry [49]. The bio-slurry is an organic-rich nutrient that intensifies the plant growth and activity of electrogenic microbes in P-MFC. The current density without bio-slurry was $114.52 \pm 20.05 \text{ mA m}^{-2}$ and $185.23 \pm 15.10 \text{ mA m}^{-2}$ for *Amaranthus viridis* and *Triticum aestivum*-based PMFC, respectively; however, it was $185.23 \pm 15.10 \text{ mA m}^{-2}$ and $291.23 \pm 7.50 \text{ mA m}^{-2}$ with bio-slurry [49]. According to Saeed et al. (2022), the power density of 60 mW m^{-3} was recorded for an Earthworm-assisted *Phragmites* plant-based P-MFC [50]. According to a recent investigation the P-MFC was used as an energy harvesting technology to amplify the 5 G signal (the fifth-generation mobile communication system). In this exploration, graphene quantum dots (GQDs) are used as catalysts to promote electricity generation in P-MFC; the system demonstrated continuous power density of 320 mW m^{-2} [51]. Thus, applying P-MFC as a bioenergy generator for different potential practical applications has a substantial futuristic scope.

2.1.2.1.4. P-MFC as biosensor. Using P-MFC as a power-generating resource still looks challenging; however, their application as biosensors has a wide scope in the near future. Recently P-MFC-based biosensors have been applied in different areas, such as bio-remediation applications, measuring the toxicity and quality of water and wastewater, plant maturity tracking sensors, and powering internet of things (IoT) devices [52]. A wireless flora health monitoring sensor was proposed in a research investigation using P-MFC, where the system was used as a power generator to provide power for supplying the wireless

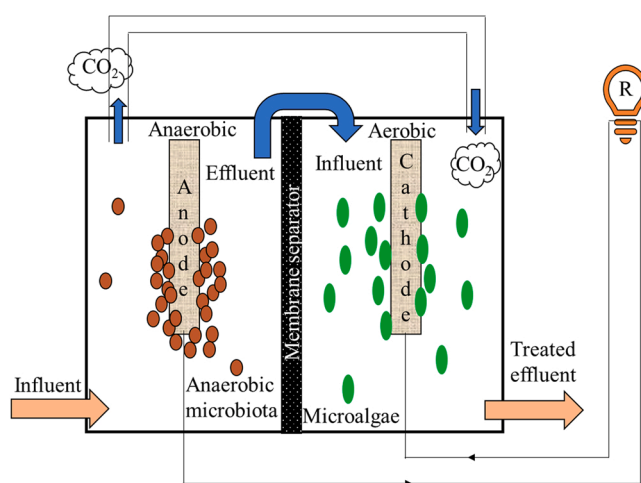


Fig. 4. Pictorial representation indicating a typical microbial carbon-capture cell.

embedded electronics and also as a biosensor to monitor the health status of the plant. The working principle of this P-MFC-based sensor is that the power rate is correlated with the health of the flora living in the symbiosis with the microbial colony [53].

In another research investigation, P-MFC was used as a power source for an ultra-low power wake-up receiver that was used as a trigger for sampling and transmitting the saved data [59]. Again, in a recent investigation, drought tolerant plants such as *Sedum* species-based P-MFC were used as a sensor to facilitate the efficient use of water for green roof irrigation. This P-MFC sensor produced a larger power density (114.6 and $82.3 \text{ } \mu\text{W m}^{-2}$ vs. $32.5 \text{ } \mu\text{W m}^{-2}$) with higher soil water content (around 27% vs. 17.5% v/v) [60]. Another exploration implemented a P-MFC array as a promising self-sustained green energy communication system for the Internet of Things-based wireless sensor network (IoT-WSN). In this demonstration, the serial-parallel arrangement of a *Dypsis lutescens* plant-based P-MFC array showed a short circuit current of 5.6 mA and an open circuit voltage of 1.75 V , respectively [52]. Thus, P-MFC-based bio-sensor indicated their utility and tremendous future in various sectors as a green energy-based technology.

2.1.3. Microbial carbon-capture cell

The MCC is an improved version of MFC, wherein photosynthetic microorganisms (algal or cyanobacteria) cultivation in the cathodic chamber facilitates CO₂ sequestration, supplies O₂ to support cathodic reduction reaction and bioenergy recovery with concurrent wastewater treatment (Fig. 4) [61]. Typically, in the anodic chamber of a MCC, anaerobic microorganisms oxidize the organic matters present in wastewater to produce CO₂. Additionally, CO₂ can be utilized by the

Table 4

Applications of MCC.

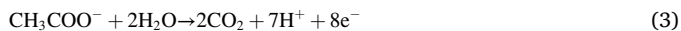
Algal species	Anode Cathode	Reactor setup Anolyte Catholyte	Applications	Results	Reference
<i>Chlorella pyrenoidosa</i>	Carbon felt Carbon felt	DCMFC Anaerobic sewage sludge in synthetic WW BG-11	Wastewater treatment, power generation, and biomass production	COD removal: 87.3 %; Power density: 6400 mW m ⁻² ; Biomass: 66.4 mg L ⁻¹ d ⁻¹	[79]
<i>Chlorococcum</i> sp.	Graphite plate graphite plate	DCMFC Kitchen WW BG-11	Power generation	Power density: 30.20 mW m ⁻²	[75]
<i>Synechococcus</i> sp.	Carbon brushes carbon cloth	Multiple anodic chambers sharing a single algal raceway pond Anaerobically digested effluent from kitchen waste as anolyte and catholyte.	Power generation	Power density: 41.48 mW m ⁻²	[80]
<i>Golenkinia</i> sp.	Carbon brushes carbon cloth			Power density: 2.34 W m ⁻³	[80]
<i>Chlorella sorokiniana</i>	Carbon felt Carbon felt	DCMFC Anaerobic sewage sludge in synthetic WW BG-11	Wastewater treatment, power generation, and biomass production	COD removal: 86.47 %; Power density: 24.09 mW m ⁻² ; Biomass: 2.1 g L ⁻¹	[81]
<i>Chlorophylla</i>	Carbon felt ZnOx-NiO@rGO carbon felt	DCMFC Synthetic anolyte Modified BG11 medium	Power generation	Power density: 31.92 mW m ⁻²	[82]
<i>Chlorella vulgaris</i>	Carbon fiber cloths Carbon fiber cloths	DCMFC Synthetic wastewater M8 medium	Power generation	Power density: 16.72 mW m ⁻²	[83]
<i>Scenedesmus quadricauda</i>				Power density: 5.96 mW m ⁻²	

Note: DCMFC- Double chamber MFC, WW- wastewater

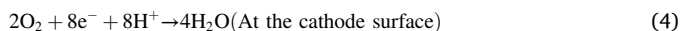
microalgae cultivated in the cathodic chamber to convert this greenhouse gas through biological conversion to valuable organic matter, such as lipids, carbohydrates, and protein [62]. Moreover, this valuable organic matter can be converted into useful products such as biodiesel, bioethanol, bio-hydrogen, and biofertilizer [63]. Furthermore, the algal cultivation in cathodic chamber generates O₂ during photosynthesis; hence, increasing the dissolved oxygen (DO) concentration and promoting the cathodic reduction reaction along with reduction in the external aeration cost as required in aqueous cathode MFC [64].

The overall bio-electrochemical reactions taking place in the anodic and cathodic chambers of the MCC are demonstrated in Eq. (3–6), respectively [65,66].

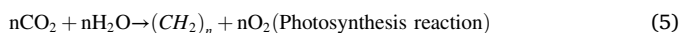
In the anodic chamber:



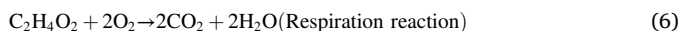
In the cathodic chamber:



Light reaction:



Dark reaction:



2.1.3.1. Applications of MCC. The objective of using algae in the cathodic chamber of MCC is to increase the DO concentration, which accelerates the ORR reaction; thus, increasing the net output power generation of the system. Moreover, MCC has many practical applications, such as wastewater treatment, biomass and bioelectricity generation, CO₂ sequestration, and many other value-added product recoveries (Table 4). The major applications of MCC are also discussed below in detail.

2.1.3.1.1. CO₂ capture and algal biomass production. The microalgae possess a specific cellular mechanism to assimilate CO₂, known as the carbon concentration mechanism (CCM). According to the CCM mechanism, a specialized cell organelle called pyrenoid increases the CO₂ concentration around the thylakoid membrane of the algal cell. The increased CO₂ concentration around the thylakoid membrane stimulates the activity of ribulose-1,5-bisphosphate carboxylase/oxygenase (known as Rubisco), an important enzyme of photosynthesis to assimilate carbon [67]. Algal cultivation not only captures CO₂; however, some investigations have been reported for flue gas, such as NO_x and SO_x capture as well [68].

The idea of algal cultivation in the cathodic chamber of MCC is

beneficial because of utilization of CO₂. Moreover, supplying CO₂ in the culture medium results in high biomass production, consequently increasing the DO concentration and improving the performance of MCC by increasing ORR as well [69]. During an operation of MCC, the maximum algal biomass concentration of 0.81 ± 0.02 mg L⁻¹ was obtained in the cathodic chamber for *Scenedesmus dimorphus* [70]. The CO₂ fixation rate of 0.085 and 0.089 g L⁻¹ d⁻¹ were found with corresponding algal biomass yields of 0.78 ± 0.05 g L⁻¹ and 1.067 ± 0.02 g L⁻¹ after 16 and 24 days of algal cultivation period, respectively [71]. Thus, applying MCC for CO₂ sequestration and algal biomass production can be a potential futuristic solution.

2.1.3.1.2. Wastewater treatment. In the anodic chamber of MCC, the exo-electrogenes utilize the organic matter present in wastewater as substrate for cellular metabolism. After anodic treatment, the anodic effluent can be treated in the cathodic chamber of MCC to remove various inorganic contaminants by algal cultivation. Wastewater from different sources like households, agricultural fields, effluent from food-processing industries, lignocellulosic waste, pharmaceutical waste, etc., can be effectively treated in MCC with simultaneous recovery of bioelectricity and other valuable products from the harvested biomass. In a recent investigation, when wastewater with 1500 mg L⁻¹ COD was treated for 10 days in the anodic chamber followed by a further treatment in the cathodic chamber of MCC with retention time of 10 days using *Chlorella vulgaris*, a total of 74 % COD removal was obtained [72]. Another investigation suggests a 72 % COD removal when real-time dairy wastewater is treated in MCC with 0.81 mg L⁻¹ *Scenedesmus dimorphus* biomass concentration [70].

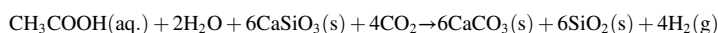
Amit et al. reported the treatment of pharmaceutical industry raw wastewater in the anodic chamber followed by aerobic microalgal treatment with *Tetraselmis indica* in the cathodic photobioreactor of MCC. The result revealed about 90.27 %, 97.05 %, 81.60 %, and 94.87 % removal of COD, TOC, nitrate, and phosphate, respectively, after 16 days of the experimental period [71]. However, when the wastewater was directly treated in the cathodic chamber of MCC, only 66.30 % of COD, 67.17 % of nitrate, 70.03 % of phosphate, and 78.14 % of TOC reduction were observed after 24 days of experiment period [71]. A comparative investigation of MCC and PMFC demonstrated the superiority of MCC over PMFC for wastewater treatment with COD, phosphate, and nitrate removal of about 57.16 %, 88.81 %, and 59.82 % for PMFC, whereas 65.27 %, 95.59 %, and 66.61 % for the MCC, respectively [73]. Thus, MCC can be considered as one of the sustainable technologies for wastewater treatment due to its higher efficiency in removing COD, nitrates, and phosphate.

2.1.3.1.3. Bio-electricity generation. Bio-electricity production with concurrent wastewater treatment and biomass production in MCC is a

sustainable goal. The electricity production in MCC depends on various bio-physico-chemical factors, such as types of bacterial inoculums present in the anodic chamber, COD of anodic and cathodic influent, pH of anolyte and catholyte, electrode materials used, PEM used, reactor design parameters, the temperature of the surrounding environment as well as the algal species and CO₂ and light intensity available for algal growth in the cathodic chamber. Though the electricity generated in a single MCC unit is insignificant for practical usage; however, it can be amplified to create higher voltage by connecting the multiple MCC units in series [74]. For the treatment of kitchen wastewater, two photosynthetic microorganisms, *Chlorococcum sp.* and *Synechococcus sp.* were cultivated in the cathodic chamber of MCC, which showed a maximum power density of 30.2 mW m⁻² and 41.5 mW m⁻², respectively [75]. According to a recent investigation, a MCC's modified cathode electrode (graphite/CuO cathode) showed better catalytic activity and led to 6 W m⁻³ of power density and 25 A m⁻³ of current density production [76]. In another investigation, the maximum current and power densities attained in an algal-assisted constructed wetland-MFC system were 235 mA m⁻³ and 33.14 mW m⁻³, respectively [77]. Again, according to Yang et al., the maximum power density produced by an algal biofilm MFC was 62.93 mW m⁻² [78].

2.1.4. Microbial electrolytic carbon capture

The MECC is a modified process of microbial electrolysis cells (MEC) for wastewater treatment with simultaneous CO₂ capture. In addition to treating wastewater, MECC also uses it as an electrolyte and energy source to dissolve base minerals, capture and transform CO₂, and generate renewable H₂ [84]. Moreover, MECC-based H₂ generated is highly pure compared to H₂ produced by the abiotic electrolysis method. In this system, wastewater is used as a microbial-assisted electrolyte; the electro-active bacteria in the anodic chamber of MECC oxidize the biodegradable contaminants present in the wastewater to generate H⁺, e⁻, and CO₂. The generated e⁻ reduce the anode (connected with an external potentiostat) and travel through an external circuit to the cathode, where water is reduced to produce H₂ and OH⁻. The H⁺ ions present in anolyte liberate metal ions (such as Ca²⁺, Mg²⁺) from waste or silicate minerals. These metal ions migrate to OH⁻-rich catholyte through PEM to form the metal hydroxide. These metal hydroxide reacts with CO₂ leading to spontaneous CO₂ sequestration to form stable carbonate and bicarbonates [85]. The overall reaction can be shown in Eq. 7:



The MECC generates H₂, making it an energy-efficient process of wastewater treatment and CO₂ capture. Moreover, being an anaerobic process, MECC creates 80 % less sludge, thus minimizing the sludge management cost. However, MECC is an endothermic process that requires an external voltage supply of 0.6–0.8 V for its operations. This voltage required can be employed from renewable sources such as MCC, MFC, P-MFC, and photocatalytic cells. To date, the MECC-related investigations have been conducted only on a lab-scale; hence, more research efforts are required to reduce the cost and improving efficiency for establishing it in a real-world application. In an investigation of MEC treating sludge hydrolysate, when mineral carbonation was integrated for CO₂ sequestration, the CH₄ content in the biogas increased by 5.1 % and reached to 95.9 %, with the CH₄ production rate improved by 16.9 %. In the same investigation the COD, protein, and polysaccharide removal were also increased by 8.4 %, 6.7 %, and 4.4 %, respectively [86].

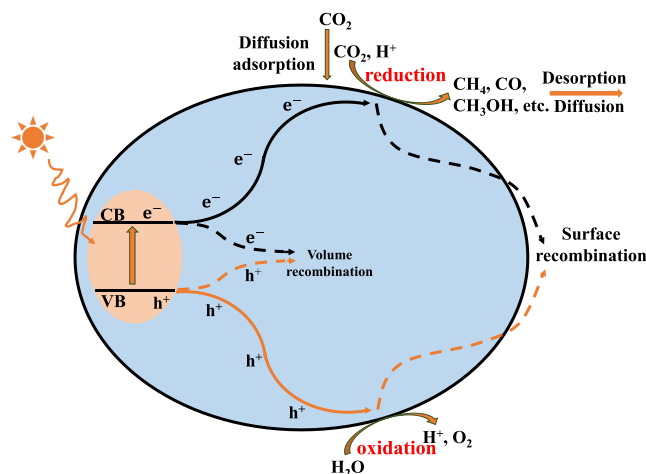


Fig. 5. Mechanism involved in the photocatalytic reduction of CO₂.

2.1.5. Application of engineered nanomaterials in METs

The main bottlenecks associated with the scaling-up of METs are low coulombic efficiency (in P-MFC and MCC) and slow rate of value-added product formed (in MES). The low coulombic efficiency and power generation are consequences of the ohmic resistance due to the electrolyte, the kinetic or charge-transfer resistance due to the slow rate of the reaction on the electrode surface, and the resistance due to retarded diffusion (transport). To deal with the problem of insufficient power densities and coulombic efficiencies, and slow rate of biochemical synthesis, electrode modification using engineered nanomaterials (ENMs) can play a significant role. The electrode should have many essential properties such as conductivity, chemical, and electrochemical stability, surface chemistry and topology, porosity, surface area, and biocompatibility that affect the electrode-microbial interaction. Electrode modification using ENMs has been considered one of the dominant approaches for microbial-electrode interaction.

Electrodes, mainly the biocathode, play a significant role in the performance of MES by providing active sites for microbial growth and conducting electron transfer [87]. Overall cell performance can be enhanced by modulating the electrode surface to increase the rate of electron transfer between the electrode and microbes [88], and this can be done by integrating nanowires or nanoparticles on the biocathode,

which reduces the activation energy related to electron transfer [89], and coating biocathodes with carbon nanotubes [89,90]. It has also been reported that modified cathode enhances the overall VFAs production [87,88,90]. Treatment of carbon cloth with gold and palladium increased the acetate production to 0.35 and 0.45 g L⁻¹, respectively [88].

In the other investigations, it has been reported that nickel nanoparticles and nanowire-coated graphite stick enhanced the generation of acetate to 0.12 g L⁻¹ and 0.54 g L⁻¹, respectively, compared to uncoated graphite cathode [89]. Overall performance of MES was improved by mounting a flexible multiwalled carbon nanotube on reticulated vitreous carbon (Nano Web-RVC) [90]. However, varied experimental conditions include electrode material, externally applied cathode potential, and the microbial population used, which have produced a wide variety of VFAs and different acetate yields. Pure autotrophic microbial strains like *Clostridium ljungdahlii*, *Sporomusa ovata*, and *Moorella thermoacetica* are primarily targeted for acetate and VFA production. Still, compared to pure culture microbial strains, mixed

Table 5
Standard redox potentials for CO₂ reduction.

Reactions	E° (V) vs SHE
$\text{CO}_2 + \text{e}^- \rightarrow \text{CO}_2^-$	-1.9
$\text{CO}_2 + 2\text{H}^+ + 2\text{e}^- \rightarrow \text{HCOOH}$	-0.61
$\text{CO}_2 + 2\text{H}^+ + 2\text{e}^- \rightarrow \text{CO} + \text{H}_2\text{O}$	-0.52
$2\text{CO}_2 + 12\text{H}^+ + 12\text{e}^- \rightarrow \text{C}_2\text{H}_4 + 4\text{H}_2\text{O}$	-0.34
$\text{CO}_2 + 4\text{H}^+ + 4\text{e}^- \rightarrow \text{HCHO} + \text{H}_2\text{O}$	-0.51
$\text{CO}_2 + 6\text{H}^+ + 6\text{e}^- \rightarrow \text{CH}_3\text{OH} + \text{H}_2\text{O}$	-0.38
$\text{CO}_2 + 8\text{H}^+ + 8\text{e}^- \rightarrow \text{CH}_4 + 2\text{H}_2\text{O}$	-0.24
$2\text{CO}_2 + 12\text{H}^+ + 12\text{e}^- \rightarrow \text{C}_2\text{H}_5\text{OH} + 3\text{H}_2\text{O}$	-0.33
$2\text{CO}_2 + 14\text{H}^+ + 14\text{e}^- \rightarrow \text{C}_2\text{H}_6 + 4\text{H}_2\text{O}$	-0.27
$3\text{CO}_2 + 18\text{H}^+ + 18\text{e}^- \rightarrow \text{C}_3\text{H}_7\text{OH} + 5\text{H}_2\text{O}$	-0.32
$2\text{H}^+ + 2\text{e}^- \rightarrow \text{H}_2$	-0.42

cultures are more versatile to environmental disturbance, possibility of operation without sterile condition, offer a higher biomass production rate [91], and convenient for future applications. Hence, it is important to utilize cultures that can efficiently produce specific organics and VFAs.

2.2. Non-biological process

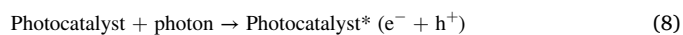
2.2.1. Fundamentals of photocatalytic-based CO₂ reduction

The photocatalytic reduction of CO₂ by semiconductor photocatalyst occurs via five consecutive steps, including absorption of light and CO₂ on the surface of catalyst, separation of charges, surface redox reaction, and desorption of product [92,93]. Initially, photons adsorbed on the surface of the catalyst to generate e^- and hole (h^+) pairs, where illumination of a semiconductor catalyst with incident light rays excites e^- from the valance band (VB), which then transfers to the conduction band (CB) by leaving an equivalent number of vacant h^+ in VB (Fig. 5) (Eq. 8). This photogenerated e^- and h^+ favour the reduction of CO₂ or oxidation of H₂O molecules. Moreover, the CB must possess more negative electrochemical redox potential (E°) than the CO₂ redox potential, and at the same time, VB should have more positive E° compared to the redox potential of H₂O (0.817 V_{SHE} at pH of 7.0) (Table 5). Therefore, the photocatalysts should have minimum band gaps to exchange e^-/h^+ pairs and utilize the solar spectrum effectively to achieve better outcomes [94]. For instance, one of the most commonly used semiconductors is TiO₂, which has a band gap of 3.2 eV that only absorbs photons from the ultraviolet (UV) domain (< 400 nm) that is present at below 5 % in the whole solar spectrum [95]. In this regard, the band gap of 1.8–2.0 eV is considered as ideal for the photoreduction of CO₂ [94]. Therefore, a strategy such as doping has been adopted to lessen the band gap of semiconductors [96].

Secondly, the separation of photogenerated e^-/h^+ pairs and charge separation depends on the prolonged lifespan of photogenerated charge carriers and their recombination rate [95]. Choosing a suitable material with high crystallinity, excellent surface properties, and band structures can overcome these two challenges. The recombination could cause a substantial loss of charge carriers and liberate energy in the form of heat. Thus, appropriate alteration of material structures by surface treatments can reduce the recombination rate and improve charge separation efficiency [97]. Third step includes adsorption of CO₂ molecules on the photocatalyst surface, wherein e^- transfer occurs between the photocatalyst and CO₂, thereby converting it to intermediates like bidentate carbonate [98]; which further get reduced to end products. Hence, the photocatalysts should have a high specific surface area to provide enhanced active sites for CO₂ adsorption.

In addition, the treatment of photocatalyst with an alkali solution can improve the photocatalyst's surface area, which can enhance the adsorption of CO₂ on the photocatalyst surface [94]. The fourth pathway involves the surface redox reactions that occur due to the photogenerated e^- and h^+ , where e^- helps to reduce CO₂ to C₁ products including, CO, CH₄, COOH₂, CH₃OH, or other hydrocarbons, while h^+

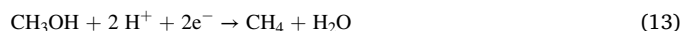
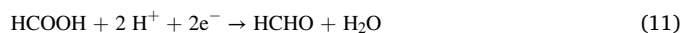
oxidizes the H₂O to molecular O₂ [95] (Eq. 9 – Eq. 13). Moreover, the addition of co-catalysts can amplify the interfacial charge transfer rate and efficiency of photocatalysts to reduce CO₂ and oxidize H₂O [97]. However, after the completion of photocatalytic reaction, product should be timely desorbed from the surface of catalyst, and the reaction then immediately terminates to avoid catalyst poisoning [94].



Oxidation reaction:



Reduction reaction:



2.2.2. Photocatalytic materials for CO₂ reduction

2.2.2.1. Metal oxides. Recently, metal oxides have been used as photocatalysts to reduce CO₂. Transition metals, such as Zr⁴⁺, Ta⁵⁺, W⁶⁺, Ti⁴⁺, and Mo⁶⁺ are generally used owing to their band structure, enabling simultaneous CO₂ reduction and oxidation of H₂O [99]. However, few have a wider band gap, which often restricts their solar spectrum utilization in the UV region [100]. Among various transition metals, titanium dioxide (TiO₂) is the most common and frequently used for the reduction of CO₂ owing to its high chemical stability, catalytic activity, low cost, abundance, and eco-friendly nature [101]. Moreover, TiO₂ naturally exists in three polymorphs, namely anatase, rutile, and brookite [102]. The anatase form receives wide attention owing to its highly active towards photocatalytic reduction of CO₂. On the other hand, the rutile form is less active due to its rapid charge recombination, while the brookite form is hardly utilized in photocatalysis because it is challenging to obtain pure-phase brookite [103].

Nevertheless, recent research recommends that pure brookite possesses an amplified catalytic activity for CO₂ reduction, as well as oxygen-deficient brookite is more effective than anatase form because of its enhanced charge transfer capability with the CO₂ molecule [103]. Apart from this, the photocatalytic ability of TiO₂ also depends upon the crystal facets. For example, the anatase TiO₂ having [010] facet has resulted in more activity, which is attributed to its more favorable surface atomic structure [104]. Similarly, transition metal oxides like zirconium oxide (ZrO₂), tungsten trioxide (WO₃), titanates (TiCl₆²⁻), and tungstate (Bi₂WO₆) have also been utilized as photocatalysts in CO₂ reduction [105,106].

Some other oxides of metal cations such as Ga³⁺, Ge⁴⁺, Sn⁴⁺, Sb⁵⁺, and In³⁺ also showed catalytic ability to reduce CO₂ owing to their hybridized sp orbitals in conduction bands, enabling the generation of photoinduced e^- with high reducing power [107]. Unfortunately, the transition metal oxides, including TiO₂, Zn₂Ga₂O₄, and ZnGeO₄, possess a high band gap of ~3.2 eV, 4.5 eV, and 4.4 eV, respectively, and their rapid hole (h^+)/electron (e^-) recombination limits the use of visible solar light (~45 %) [108,109]. Thus, hybridization techniques can be adopted to harvest visible light and reduce the recombination rate of catalyst.

2.2.2.2. Metal sulfides. Recently, metal sulfide emerged as a new set of photocatalysts to reduce CO₂ owing to having higher VB and narrower band gaps compared to metal oxides. However, the h^+ generated on their VB do not have adequate capability to oxidize the water molecules, resulting in irreversible photo-corrosion in the system. Thus, to avoid

Table 6
Summary of photocatalytic reduction of CO₂.

Photocatalysts	Light source	Major products	Yield of products	Reference
Cu/TiO ₂ -SiO ₂	Xe lamp	CO CH ₄	60 μmol g-cat ⁻¹ h ⁻¹ 10 μmol g-cat ⁻¹ h ⁻¹	[114]
Graphene oxides	Halogen lamp	CH ₃ OH	0.172 mmol g-cat ⁻¹ h ⁻¹	[115]
CNT-Ni/TiO ₂	Visible daylight lamp	CH ₄	0.145 mmol g-cat ⁻¹ h ⁻¹	[116]
Montmorillonite modified TiO ₂	Hg lamp	CH ₄	441.5 mmol g-cat ⁻¹ h ⁻¹	[117]
SnO _{2-x} /g-C ₃ N ₄	Xe lamp	CH ₃ OH	22.7 μmol g-cat ⁻¹ h ⁻¹	[118]
Graphene-Ti _{0.91} O ₂ hollow spheres	Xe lamp	CO CH ₄	9 μmol h ⁻¹ g ⁻¹ 1 μmol h ⁻¹ g ⁻¹	[119]
Bi ₂ WO ₆	Xe lamp	CH ₃ OH	502 μmol g ⁻¹ h ⁻¹	[120]
Zn ₂ GeO ₄ nanobelts	Xe lamp	CH ₄	6 μmol h ⁻¹ g ⁻¹	[108]
CeO ₂	Xe lamp	CH ₄	1.12 μmol h ⁻¹ g ⁻¹	[121]
Cu ₂ S nanorod	Xe lamp	CO CH ₄	3.02 μmol h ⁻¹ g ⁻¹ 0.13 μmol h ⁻¹ g ⁻¹	[122]
In ₂ O ₃ /BiOI with type II heterojunctions	Xe lamp	CO CH ₄	11.98 μmol h ⁻¹ g ⁻¹ 5.69 μmol h ⁻¹ g ⁻¹	[123]
Bi ₂ S ₃	Hg lamp	HCOOH	700 μmol g ⁻¹ (4 h)	[124]
MIL-101(Fe)	Visible light	HCOO ⁻	7.375 μmol h ⁻¹	[125]
Co-ZIF-9	Visible light	CO	28.54 μmol h ⁻¹	[111]
NH ₂ -UiO-66(Zr)	Visible light	HCOO ⁻	1.32 μmol h ⁻¹	[126]

photo-corrosion, hole scavengers are often added to enhance the stability of metal sulfide. In 1988, Eggins and co-workers, for the very first time, utilized CdS as a photocatalyst to generate formaldehyde, methanol, formate, acetate, and glyoxylate from the reduction of CO₂ under visible light irradiation [110]. Recently, Wang and Wang achieved CO from the photoreduction of CO₂ by using CdS coupled with Co-ZIF-9 as the cocatalyst under monochromatic radiation [111].

Similarly, ZnS also received significant attention from researchers for the photocatalytic reduction of CO₂ due to having very high energy in the CB and low redox potential of -1.8 to -2.0 V_{SHE}, that could enable one-electron reduction of CO₂ to CO₂^{•-} as verified by electron spin resonance analysis and radicals scavenging experiments [111]. Furthermore, Baran and co-workers identified the formation of formic acid, CO, and a trace amount of methane as the primary end products during the photocatalytic reduction of CO₂ with ZnS nanoparticles functionalized with Ru cocatalyst [112]. Consequently, they also found that photocatalytic activity depends on nanoparticle size and solvent polarity. In another investigation, the formation of carboxylic acid was observed during the photocatalyzed reduction of CO₂ by ZnS [113]. Similarly, other researchers have reported the successful application of metal sulfides and their composites as photocatalysts to reduce CO₂, as presented in Table 6.

2.2.2.3. Metal-Organic frameworks. Most recently, metal organic frameworks (MOFs), a new group of highly porous materials consisting of metal nodes interconnected with organic linkers, have received much attention owing to their extraordinary chemical and functional versatility, large specific surface area, tunable pore structure, high conductivity and high density of active sites [127,128]. Most uniquely, MOFs contain catalytic centers and photosensitizers in a single solid, which is a

promising alternative to conventional semiconductors for photocatalysis. For instance, the metal nodes and organic linkers of many Ti-based MOFs have a high photocatalytic ability due to titanium oxide (TiO₂) clusters, which can easily absorb the light and activate under UV-vis radiation.

In 2012, Fu and co-workers, for the first time, reported the photocatalytic reduction of CO₂ to formate under visible light radiation using Ti-containing MIL-125-NH₂ with 2-aminoterephthalate organic linker as the photocatalyst [129]. Similarly, in another investigation, Logan and co-workers prepared MIL-125-NH₂(Ti), where the amine functionality was decorated with alkyl chains that attributed mainly in the narrowing of the bandgap of MOF from 2.56 to 2.29 eV; thereby, enhanced photocatalytic reaction rates and quantum yield for reducing CO₂ to formate [130]. Similarly, as presented in Table 6, other metal-based MOFs have been utilized successfully as photocatalysts for the reduction of CO₂.

2.2.2.4. Carbonaceous material. Reducing CO₂ using carbonaceous materials has attracted their utilization by their advantages like biocompatibility, conductivity, chemical stability, large surface area, and low cost [131]. Despite of other advantages, pristine carbonaceous materials are generally inert and possess very negligible catalytic activity for CO₂ reduction. Thus, the carbonaceous materials are properly doped with heteroatoms (e.g., N, B, P, and S) to introduce structural defects or to enhance the charge spin densities on the adjacent carbon atoms, which can significantly alter the interaction of carbonaceous materials with CO₂ or reaction intermediates. For example, heteroatom functionalized carbonaceous materials, such as carbon nanotubes (CNTs), graphene sheets, carbon nanofibers (CNFs), and graphitic carbon nitride (g-C₃N₄) and graphene quantum dots have been utilized in CO₂ reduction. Among them, g-C₃N₄ possesses good catalytic ability owing to its layered structure and tri-s-triazine units [132].

In 2013, for the very first time, Mao and co-workers investigated the photocatalytic reduction of CO₂ using C₃N₄ and observed the yielding of methanol and ethanol from the porous C₃N₄ derived from urea and only ethanol from nonporous C₃N₄ derived from melamine [133]. In another investigation, Kuriki and co-workers achieved formic acid from the reduction of CO₂ using a C₃N₄-Ru composite [134]. Similarly, Shi and co-workers observed that the exfoliated C₃N₄ nanosheets and Zr-based MOF (UiO-66) composite showed better charge separation capability and prolonged lifetime of photogenerated carriers [135]. Also, a higher photocatalytic activity for CO₂ reduction to CO (9.9 μmol g⁻¹ h⁻¹) was observed under visible light irradiation [135].

2.2.3. Fundamentals of electrochemical CO₂ reduction

In the electrochemical reactor, CO₂ can be directly supplied in a gas phase medium for its reduction at the cathode, which is also known as direct electrochemical reduction of gaseous CO₂ (DERC). The DERC occurs at the cathode to generate carbon monoxide (CO), formic acid (HCOOH), methane (CH₄), ethylene (C₂H₄), and many other hydrocarbons as value-added products depending on the nature of electrocatalysts, applied potential and electrolyte medium (Fig. 6a) [136,137]. Initially, the CO₂ gets converted to CO₂^{•-} radical via an electron transfer mechanism, which is further reduced via the protonation of its oxygen atom and form [•]COOH [138,139]. On the other hand, the reduction of CO₂^{•-} via protonation of its carbon atom at high overpotentials can produce HCOO[•] instead of [•]COOH, which can further be reduced to formate (HCOO⁻) [94].

Moreover, the transformation of CO₂ into multi-carbon (C₂₊) products has attracted considerable attention because of their higher energy density and market value. However, compared with C₁ products, the yield of C₂₊ products (i.e., C₂H₄, C₂H₅OH) is relatively low because of their poor C₂₊ selectivity at high CO₂ conversion rates [140,141]. In this regard, several strategies, including morphology and facet engineering, dopant modification, bimetallic catalysis, and electrolyte design have been established to boost the efficacy of catalysts for C₂₊ product

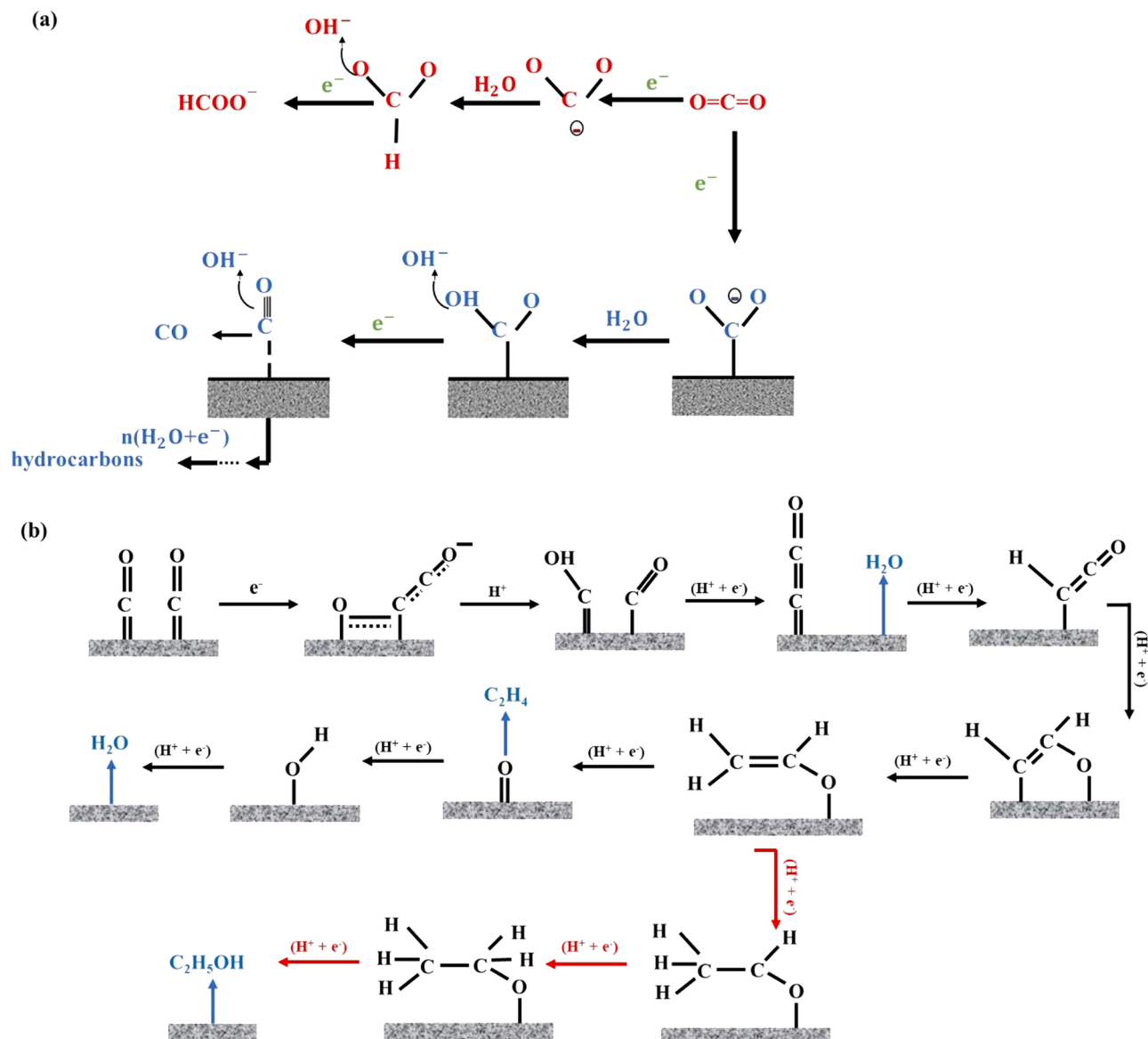


Fig. 6. (a) Mechanism involved in the production of valuables via electrocatalytic reduction of CO₂, (b) pathways of transformation of CO₂ to ethylene (C₂H₄) and ethanol (C₂H₅OH).

Table 7
Summary of electrocatalytic reduction of CO₂.

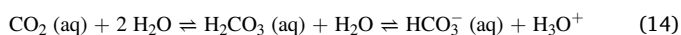
Electrocatalyst	Electrolyte	E° (V) vs SHE	Major Product	Faradaic efficiency (FE) (%)	Current Density (mA cm ⁻²)	Reference
Cu NPs	0.1 M KHCO ₃	- 1.1	H ₂ CO CH ₄ C ₂ H ₄	-	20	[146]
Mesostructured Ag	0.1 M KHCO ₃	- 0.7	CO	> 80	-	[147]
Sn NPs/graphene	0.1 M NaHCO ₃	- 1.8	HCOOH	93.6	10.2	[148]
Cu-In	0.1 M KHCO ₃	- 0.5	CO	90	0.53	[149]
WSe ₂	50 mol % water and 50 mol % 1-ethyl-3-methylimidazolium tetrafluoroborate (EMIM-BF ₄)	- 0.76	CO	85	330	[150]
N-doped graphene quantum dots (QDs)	1 M KOH	- 0.86	C ₂ H ₄ C ₂ H ₅ OH CO	90	100	[151]
MoS ₂	96 mol % water and 4 mol % EMIM-BF ₄	- 0.764	CO	98	65	[152]

Table 8Application of abiotic-biotic hybrid system for CO₂ reduction to produce methane.

Hybrid system	Culture	Energy source	Pathway	CH ₄ production rate	Reference
M. barkeri -CdS biohybrid	<i>Methanosarcina barkeri</i>	Solar energy	DET and H ₂ -mediated ET	4.6 μmol day ⁻¹	[156]
Microbial-photoelectrochemical hybrid system	<i>Methanogenic</i> communities	Solar energy	DET and H ₂ -mediated ET	4.2 μmol cm ⁻² day ⁻¹	[158]
M. barkeri -Ni (0.75 %):CdS biohybrid	<i>Methanosarcina barkeri</i>	Solar energy	DET and H ₂ -mediated ET	6 μmol day ⁻¹	[159]
Electrode-archaea hybrid	Co-culture (<i>Methanococcus maripaludis</i> and <i>Acetobacterium woodii</i>)	Imposed potential (−0.5 V vs. SHE)	DET and H ₂ -mediated ET	18 μmol cm ⁻² day ⁻¹	[160]
GO/PEDOT modified electrode-archaea hybrid	<i>Methanogenic</i> communities	Imposed potential (−0.9 V vs. Ag/AgCl)	DET and H ₂ -mediated ET	32 μmol cm ⁻² day ⁻¹	[161]

Note: PEDOT- Poly (3,4-ethylenedioxythiophene), DET- Direct electron transfer, ET- Electron transfer

formation [142]. For instance, in an investigation, a Cu–Ag alloy catalyst with active bimetal centers was used to improve the selectivity of CO₂ for C₂H₅OH (Fig. 6(b)) [140]. Herein, the highly coordinated surface of the Cu nanoparticle encouraged the binding of unsaturated reaction intermediates of C₂H₄ over C₂H₅OH, whereas the Ag nanoparticle helped to destabilize the C₂H₄ intermediates. Thereby, the synergetic effect of Cu and Ag active centers promoted the production of C₂H₅OH [140]. Therefore, most CO₂ reduction electrocatalysts form CO or formate as the end reduction products instead of hydrocarbons [143]. Moreover, the interaction of CO₂ with H₂O produces a complex series of reversible reactions (Eq. 14 - Eq. 15). A more detailed mechanism involved in electrochemical CO₂ reduction was provided by Li et al. [144] and Jones et al. [145].



During CO₂ reduction in aqueous media, some of the metal catalysts, such as Pt, Ti, Ni and Fe evaluate hydrogen via hydrogen evolution reaction (HER), which competes with CO₂ reduction. Thus, to avoid HER, catalysts with high HER overpotentials are often chosen to reduce CO₂. In this regards, numerous catalyst materials, such as metals, metal chalcogenides and carbonaceous materials, have been developed and utilized as electrocatalysts for the efficient reduction of CO₂ (Table 7).

Thus, the above investigations showed that photocatalysts, such as metals, metal chalcogenides, metal oxides, metal sulfides, MOFs, and carbonaceous materials, could reduce the CO₂ to valuable end products. However, one obvious limitation is carbon contamination, which occurs due to the organic substances like solvents, reactants, and surfactants involved during the catalyst preparation increasing the carbonaceous residues in the final product. Later, the residues decompose into CO and CH₄, which can cause the overestimation of catalytic activities [103]. Therefore, it is necessary to confirm that the measured products are generated from the reduction of CO₂ rather than the decomposition of carbonaceous residues. Moreover, the isotopic ¹³CO₂ labeling method has been employed in many investigations to verify the origin of reduced end products. In addition, the possible ways of carbon contamination can also be identified by carrying out the control experiments under identical operating conditions [94].

3. Hybrid technologies for CO₂ reduction

In the recent years, abiotic and biotic hybrid systems, wherein natural biocatalyst with high reduction selectivity and abiotic catalyst with high efficiency for electricity/solar driven reduction of CO₂ have gained much attention of the researchers. The CO₂ reduction through hybrid technologies can be achieved in two ways: (i) microbial electro-synthesis technologies that use electricity to support whole-cell biological CO₂ reduction to target products and (ii) photo-catalyst based bio-hybrid nanomaterials with CO₂-fixing microbes to harness solar energy for biological CO₂ transformation into value added products [153]. High energy conversion efficacy and short reaction time are the advantages of using abiotic catalyst for CO₂ reduction. However, long carbon-chain

forming reactions for reduction of CO₂ is not easily achieved with abiotic catalyst owing to the requirement for high activation energy for transforming thermodynamically stable CO₂ molecule into valuable fuel [154]. Additionally, electrochemical reduction of CO₂ requires high external energy for its operation, which is the main disadvantage of this technology.

On the other hand, long chain products can be obtained by CO₂ fixation pathways in biological systems. In biological transformation, CO₂ is primary reduced and bio-transformed to acyl-CoA dehydrogenases (Co-enzyme that metabolize fatty acid). Subsequently, long chain carbon products were formed with the oxidation of fatty acids owing to the catalyzed action of acyl-CoA [155]. Thus, long chain products, such as limonene, farnesene and isoprene, were produced via biological transformation of CO₂. Moreover, biological transformation of CO₂ is advantageous as it requires mild reaction condition and lower applied potential (in case of MEC), low substrate activation barrier and high product selectivity [153]. Thus, hybrid photo/electrochemical process with biological systems can offer sustainable solution for conversion of CO₂ into value added products.

In this regard, Bai and co-workers utilized carbon nanotubes – *Methanosarcina barkeri* (Archaea) based hybrid system in bio-electrochemical setup for the transformation of CO₂ [156]. The authors reported about 4.4 μmol cm⁻² day⁻¹ of methane production rate at an applied voltage of −1.2 V during 72 h of retention time via direct and H₂ mediated indirect electron transfer [156]. Moreover, at an applied potential of −0.35 V lower methane production was obtained (0.04 μmol) during 72 h of retention time, which can be due to no H₂ production at an applied potential of −0.35 V for H₂ mediated indirect electron transfer [156]. Hence, only direct electron transfer contributed in the methane production at an applied potential of −0.35 V. Thus, a lower removal was reported.

Additionally, Kracke et al. reported about 1.4 L per day of methane production rate from CO₂ with NiMo-graphite cathodes and pure cultures of hydrogenotrophic *Methanococcus maripaludis* in bio-electrochemical system at an applied potential of −0.65 V [157]. Moreover, the operation has resulted in more than 90 % of coulombic efficiency for 4 weeks of operation; thereby, revealing high stability and performance of the bioelectrochemical technology for CO₂ reduction [157]. The high performance can be attributed to a more efficient utilization of in situ produced H₂ owing to the application of −0.65 V applied potential compared to externally added gaseous H₂ [157]. Thus, H₂ mediated electron transfer occurs and efficient methane is recovered from the system. Moreover, natural photosynthesis was also utilized for CO₂ conversion into value-added products, and solar energy driven photoanode (TiO₂)-photocathode (InP/Pt)-*M. barkeri* hybrid system was operated for methane production. The photocatalyst-based hybrid system demonstrated 8 nmol cm⁻² day⁻¹ production rate of methane over 7 days of retention time with 86 % of Faradic efficiency following H₂ mediated electron transfer mechanism. Similar other research reports pertaining to the production of methane through CO₂ reduction using abiotic-biotic hybrid system are presented in Table 8.

Table 9

Advantages and disadvantages of biological and non-biological CO₂ sequestration technologies.

Technology	Advantages	Disadvantages	Technology readiness level (TRL)	Example of projects, year and location	Products obtained	Reference
Biological	<ul style="list-style-type: none"> Requires less energy for carbon capture, Utilization of plant, algae and microbes is cost-effective Direct injection of CO₂ can be possible for enhancing the productivity 	<ul style="list-style-type: none"> Less harvesting of valuables due to low adsorption capacity largely relies on the climatic condition 	4 (microalgal) 4–7 (photosynthetic)	<ul style="list-style-type: none"> ALGAENET (2012), Madrid – Spain PhotoFuel (2015), Wolfsburg – Germany Algenol (2010), IBRFlorida – US BioPower2Gas (2013), Allendorf – Germany 	Biogas Biofuels Bioethanol Methane	[141, 167]
Photochemical	<ul style="list-style-type: none"> High yield of products Requires mild operating conditions Easy alteration of operating parameters Consume less energy 	<ul style="list-style-type: none"> Separation of product and catalyst is difficult Design of photoreactor is costly and complex Product selectivity is a major drawback 	2–4	<ul style="list-style-type: none"> PROPHCEY (2016), Karlsruhe -Germany 	C ₁ chemicals	[141]
Electrochemical	<ul style="list-style-type: none"> Operates in room temperature Valuables recovered can be used as source for power production Scaling up is easy. 	<ul style="list-style-type: none"> High cost of electrode materials High operational cost Electrode fouling Slow kinetics 	2–4 (for C ₂ + production) 2 (for C ₁ production)	<ul style="list-style-type: none"> CELBICON (2016), Turin – Italy LOTTER.CO2M (2018), Cologne – Germany Rheticus (2018), Marl – Germany 	Syngas, formic acid Methanol Butanol, hexanol	[141, 168]
Chemical	<ul style="list-style-type: none"> Direct CO₂ is used as a raw material Products including carboxylic acid, urea and dimethyl carbonate are formed during this conversion 	<ul style="list-style-type: none"> Utilization of CO₂ less High operational cost 	7–9 (Mineralization)	<ul style="list-style-type: none"> MCI (2013), Newcastle – Australia SkyMine® (2010), Texas – USA SOLID Life (2016), Weimar – Germany 	Inorganic carbonates Sodium bicarbonate NA	[141]
Thermochemical	<ul style="list-style-type: none"> Production of syngas (H₂ and CO) through thermal reforming, which can be transformed into potent liquid fuel 	<ul style="list-style-type: none"> High energy and temperature are required Instability of the catalyst Fuel formation is risky 	4 (Methanol) 4–6 (Reforming)	<ul style="list-style-type: none"> Shell-Sari-Lu'An joint (2011), Shanxi Province – China Sunexus CO₂ reforming (2010), California – USA 	Syngas Syngas, diesel	[141]

4. Readiness level and cost assessment of CO₂ reduction technologies

The maturity of the CO₂ transformation technologies is measured by the technology readiness level (TRL) tool as shown in Table 9. The photochemical transformation technique is categorized with a TRL level of 2–4, since this technology is still being corroborated at the lab-scale [162]. On the other hand, non-photosynthetic processes as well as electrochemical reduction have been attributed with a readiness level of 3–5, as these processes are explored at a pilot level in mega projects of CO₂ reduction like BioPower2Gas. In addition, photosynthetic, reforming, and mineralization technologies have a more mature TRLs of 4–7, 4–6, and 7–9, respectively [141,163]. Technologies like carboxylation and hydrogenation have a broad range TRL between 2 and 9 because a wide variety of products that can be obtained [141]. For instance, in case of carboxylation, urea can be produced (TRL 7–9), similarly with hydrogenation formic acid can be recovered (TRL 3–5) [164].

Another important aspect for the real scale deployment of CO₂ reduction technologies is the cost assessment, which includes capital and operational expenditures. Capital cost is mainly attributed to designing, buying equipment's, and building the treatment plant. Whereas operational costs consist of plant maintenance and operations (fixed cost) and for raw materials like utilities, catalyst and disposal of by-products (variable cost). The utilities for operating a treatment system can be electrical energy, heating, and cooling consumption. For instance, the capital cost, operational cost, and energy consumption of about 805.7 US\$, 1016.13 US\$ and 1.1 MWh; respectively, were obtained for per ton electrochemical reduction of CO₂ to formic acid with a plant life of 25 years [165]. Similarly, in the case of photosynthetic conversion of CO₂, about 494.22 US\$, 1724.72–2624.37 US\$, and 1.6 MWh of capital cost, operational cost, and energy consumption were reported for the production of per ton of algal oil, respectively [166]. Important aspects for the real scale deployment of CO₂ reduction technologies are shown in the Table 9.

5. Conclusion and future perspectives

Global warming and a huge amount of wastewater generation due to anthropogenic activity is a pivotal problem for present and future generations. The most effective way to minimize global warming is the preventive measure to limit CO₂ and other greenhouse gas production and release to atmosphere. However, wastewater generation can be minimized by reducing the use of toxic chemicals in our daily life. To effectively enforce preventive measures, alternative sustainable approaches should be explored and applied in everyday life; e.g., promoting the use of CNG or solar-based vehicles instead of petroleum-based, use of natural pesticides instead of synthetic pesticides. Although complete replacement cannot be applied suddenly, however reduction in the use of toxic chemicals and greenhouse gas producing appliances can reduce the environmental burden. Therefore, the most effective way to minimize global warming and wastewater generation in the present and future is the proper use of available resources. In addition to source monitoring and control, the CO₂ capture and wastewater treatment are the demand of the current era. Different types of biological and non-biological CO₂ capture technologies are available, which have been discussed in this manuscript. Considering the present developments, both biological and non-biological processes have shown excellent results in CO₂ capture. However, numerous obstacles still need to be addressed for the successful practical implementation of these technologies, which are highlighted below in detail.

In case of photocatalytic reduction process, detail techno-economic analysis is required to be performed to estimate the production cost of chemical fuels from CO₂ reduction. Moreover, poor photocatalytic efficiency due to less responsive to sunlight and high recombination rate of photo-generated species are the major limitations responsible for low productivity in photocatalytic reduction of CO₂. Therefore, future

exploration should be directed towards to find novel visible-light-responsive photo-catalysts with a wide band gap, which can accelerate the rate of photo-generated e^-/h^+ transport, and reduce the rate of recombination. For electro-catalytic reduction process, low-cost and more durable catalysts are required to be developed via simple synthesis methods, which could aid in large-scale synthesis and enhance the crystallinity, structure, surface morphology, and size of the catalysts. In addition, the understanding of reaction pathway and mechanism involved in CO₂ reduction in both the processes are still missing at this moment. Thus, a clear understanding on how CO₂ adsorbed, transformed and desorbed during CO₂ reduction process is required to be investigated in detail through the advanced electronic and spectroscopic tools like transmission electron microscopy (TEM), X-ray absorption spectroscopy (XAS), electron spin resonance (ESR) and time-resolved fluorescence (TRF) spectroscopy.

On the other hand, METs have also massive potential in bioenergy generation and valuable product synthesis and recovery. These techniques are capable of treating low as well as high-strength wastewaters. The METs can be considered as an emerging sustainable technology that can be operated in inaccessible areas with minimum human intervention. Among METs, the MCC can be considered more sustainable in terms of its diverse applications; it has comparatively superior potential for CO₂ sequestration and nutrient removal and produces valuable photosynthetic microbial biomass. Being an algae-based system, it is also applicable in removing antibiotics and other emerging contaminants. Moreover, algal biomass has huge applications, such as biodiesel production, bioethanol production, source of many secondary metabolites, biochar production, and use as animal feed. Apart from the advantages associated with MCC, it has limitation of generating low output power. Therefore, more research is required to improve the power generation by MCC. The low-cost biocompatible conductive nanocatalyst based-electrode, high permeable PEM, and selection of highly growing electrogenic bacterial inoculum and algal inoculum might be the solution for low power generation in MCC. Although much research on MCC has been conducted to date, a successful field-scale application of this technology has not been achieved yet. Thus, successful up-scaling of this technology is required to be developed after addressing the associated limitations.

CRedit authorship contribution statement

Santosh Kumar: Conceptualization, Visualization, Validation, Writing – original draft, Writing – review & editing, Software support, Formal analysis, and Investigation. **Monali Priyadarshini:** Conceptualization, Visualization, Validation, Writing – original draft, Data curation, Writing – review & editing, Investigation. **Azhan Ahmad:** Software, Visualization, Writing – original draft, Writing – review & editing. **M.M. Ghangrekar:** Resources, Funding acquisition, Supervision, Project administration, Writing – review & editing.

Declaration of Competing Interest

The authors declare that they have no known competing financial interests or personal relationships that could have appeared to influence the work reported in this paper.

Data Availability

Data will be made available on request.

Acknowledgements

The fellowship received for first author from the Ministry of New and Renewable Energy, Government of India (IIT/SRIC/R/REF/2018/101) is duly acknowledged.

References

- [1] J. Meng, X. Hu, P. Chen, D.M. Coffman, M. Han, The unequal contribution to global energy consumption along the supply chain, *J. Environ. Manag.* 268 (2020), 110701, <https://doi.org/10.1016/j.jenvman.2020.110701>.
- [2] M. Woydt, The importance of tribology for reducing CO₂ emissions and for sustainability, *Wear* 474–475 (2021), 203768, <https://doi.org/10.1016/j.wear.2021.203768>.
- [3] S. Reen, K. Wayne, H. Yi, S. Ho, H. Siti, H. Munawaroh, P. Loke, CO₂ mitigation and phycoremediation of industrial flue gas and wastewater via microalgae-bacteria consortium: Possibilities and challenges, *Chem. Eng. J.* 425 (2021), 131436, <https://doi.org/10.1016/j.cej.2021.131436>.
- [4] C. Sepulveda, C. Gómez, N.E.L. Bahraoui, G. Acién, Comparative evaluation of microalgae strains for CO₂ capture purposes, *J. CO₂ Util.* 30 (2019) 158–167, <https://doi.org/10.1016/j.jcou.2019.02.004>.
- [5] B. Kumar, J.P. Brian, V. Atla, S. Kumari, K.A. Bertram, R.T. White, J.M. Spurgeon, New trends in the development of heterogeneous catalysts for electrochemical CO₂ reduction, *Catal. Today* 270 (2016) 19–30, <https://doi.org/10.1016/j.cattod.2016.02.006>.
- [6] B. Zhang, Y. Jiang, M. Gao, T. Ma, W. Sun, H. Pan, Recent progress on hybrid electrocatalysts for efficient electrochemical CO₂ reduction, *Nano Energy* 80 (2021), 105504, <https://doi.org/10.1016/j.nanoen.2020.105504>.
- [7] S. Zhao, S. Li, T. Guo, S. Zhang, J. Wang, Y. Wu, Advances in Sn - based catalysts for electrochemical - CO₂ reduction, *Nano-Micro Lett.* 11 (2019) 1–19, <https://doi.org/10.1007/s40820-019-0293-x>.
- [8] Q. Hu, Z. Han, X. Wang, G. Li, Z. Wang, X. Huang, H. Yang, X. Ren, Q. Zhang, J. Liu, C. He, Facile synthesis of sub-nanometric copper clusters by double confinement enables selective reduction of carbon dioxide to methane, *Angew. Chem. Int. Ed.* 518060 (2020) 19054–19059, <https://doi.org/10.1002/anie.202009277>.
- [9] I. Masood ul Hasan, L. Peng, J. Mao, R. He, Y. Wang, J. Fu, N. Xu, J. Qiao, Carbon-based metal-free catalysts for electrochemical CO₂ reduction: activity, selectivity, and stability, *Carbon Energy* 3 (2021) 24–49, <https://doi.org/10.1002/cey2.87>.
- [10] S. Das, L. Diels, D. Pant, S.A. Patil, M.M. Ghangrekar, Review—microbial electrosynthesis: a way towards the production of electro-commodities through carbon sequestration with microbes as biocatalysts, *J. Electrochem. Soc.* 167 (2020), 155510, <https://doi.org/10.1149/1945-7111/abb836>.
- [11] S. Das, S. Das, I. Das, M.M. Ghangrekar, Application of bioelectrochemical systems for carbon dioxide sequestration and concomitant valuable recovery: a review, *Mater. Sci. Energy Technol.* 2 (2019) 687–696, <https://doi.org/10.1016/j.mset.2019.08.003>.
- [12] X. Christodoulou, T. Okoroafor, S. Parry, S.B. Velasquez-Orta, The use of carbon dioxide in microbial electrosynthesis: advancements, sustainability and economic feasibility, *J. CO₂ Util.* 18 (2017) 390–399, <https://doi.org/10.1016/j.jcou.2017.01.027>.
- [13] M. Zhou, M. Chi, J. Luo, H. He, T. Jin, An overview of electrode materials in microbial fuel cells, *J. Power Sources* 196 (2011) 4427–4435, <https://doi.org/10.1016/j.jpowsour.2011.01.012>.
- [14] S. Zhang, J. Jiang, H. Wang, F. Li, T. Hua, W. Wang, A review of microbial electrosynthesis applied to carbon dioxide capture and conversion: the basic principles, electrode materials, and bioproducts, *J. CO₂ Util.* 51 (2021), 101640, <https://doi.org/10.1016/j.jcou.2021.101640>.
- [15] M. Sharma, Y. Alvarez-Gallego, W. Achouak, D. Pant, P.M. Sarma, X. Dominguez-Benetton, Electrode material properties for designing effective microbial electrosynthesis systems, *J. Mater. Chem. A* 7 (2019) 24420–24436, <https://doi.org/10.1039/C9TA04886C>.
- [16] T. Song, T. Li, R. Tao, H.F. Huang, J. Xie, CuO/g-C₃N₄ heterojunction photocathode enhances the microbial electrosynthesis of acetate through CO₂ reduction, *Sci. Total Environ.* 818 (2022), 151820, <https://doi.org/10.1016/j.scitotenv.2021.151820>.
- [17] S. Das, S. Das, M.M. Ghangrekar, Application of TiO₂ and Rh as cathode catalyst to boost the microbial electrosynthesis of organic compounds through CO₂ sequestration, *Process Biochem* 101 (2021) 237–246, <https://doi.org/10.1016/j.procbio.2020.11.017>.
- [18] Y. He, Q. Li, J. Li, L. Zhang, Q. Fu, X. Zhu, Q. Liao, Magnetic assembling GO/Fe₃O₄/microbes as hybridized biofilms for enhanced methane production in microbial electrosynthesis, *Renew. Energy* 185 (2022) 862–870, <https://doi.org/10.1016/j.renene.2021.12.117>.
- [19] M. Quraishi, K. Wani, S. Pandit, P.K. Gupta, A.K. Rai, D. Lahiri, D.A. Jadhav, R. Ray, S.P. Jung, V.K. Thakur, R. Prasad, Valorisation of CO₂ into value-added products via microbial electrosynthesis (MES) and electro-fermentation technology, *Fermentation* 7 (2021) 291, <https://doi.org/10.3390/fermentation7040291>.
- [20] S. Li, Y.E. Song, J. Baek, H.S. Im, M. Sakuntala, M. Kim, C. Park, B. Min, J.R. Kim, Bioelectrosynthetic conversion of CO₂ using different redox mediators: electron and carbon balances in a bioelectrochemical system, *Energies* 13 (2020) 2572, <https://doi.org/10.3390/en13102572>.
- [21] P. Dessi, L. Rovira-Alsina, C. Sánchez, G.K. Dinesh, W. Tong, P. Chatterjee, M. Tedesco, P. Farràs, H.M.V. Hamelers, S. Puig, Microbial electrosynthesis: towards sustainable biorefineries for production of green chemicals from CO₂ emissions, *Biotechnol. Adv.* 46 (2021), 107675, <https://doi.org/10.1016/j.biotechadv.2020.107675>.
- [22] K. Rabaey, P. Girguis, L.K. Nielsen, Metabolic and practical considerations on microbial electrosynthesis, *Curr. Opin. Biotechnol.* 22 (2011) 371–377, <https://doi.org/10.1016/j.copbio.2011.01.010>.
- [23] L. Jourdin, T. Burdyny, Microbial electrosynthesis: where do we go from here, *Trends Biotechnol.* 39 (2021) 359–369, <https://doi.org/10.1016/j.tibtech.2020.10.014>.
- [24] J.E. Reiner, K. Geiger, M. Hackbarth, M. Fink, C.J. Lapp, T. Jung, A. Dötsch, M. Hügler, M. Wagner, A. Hille-Reichel, W. Wilcke, S. Kerzenmacher, H. Horn, J. Gescher, From an extremophilic community to an electroautotrophic production strain: identifying a novel *Knallgas bacterium* as cathodic biofilm biocatalyst, *ISME J.* 14 (2020) 1125–1140, <https://doi.org/10.1038/s41396-020-0595-5>.
- [25] L. Yu, Y. Yuan, J. Tang, S. Zhou, Thermophilic *Moorella thermoautotrophica*-immobilized cathode enhanced microbial electrosynthesis of acetate and formate from CO₂, *Bioelectrochemistry* 117 (2017) 23–28, <https://doi.org/10.1016/j.bioelechem.2017.05.001>.
- [26] L. Rovira-Alsina, E. Perona-Vico, L. Bañeras, J. Colprim, M.D. Balaguer, S. Puig, Thermophilic bio-electro CO₂ recycling into organic compounds, *Green. Chem.* 22 (2020) 2947–2955, <https://doi.org/10.1039/D0GC00320D>.
- [27] A. Gomez Vidales, G. Bruant, S. Omanovic, B. Tartakovsky, Carbon dioxide conversion to C1 - C2 compounds in a microbial electrosynthesis cell with in situ electrodeposition of nickel and iron, *Electrochim. Acta* 383 (2021), 138349, <https://doi.org/10.1016/j.electacta.2021.138349>.
- [28] X. Li, S. Chen, D. Liang, M. Alvarado-Morales, Low-grade heat energy driven microbial electrosynthesis for ethanol and acetate production from CO₂ reduction, *J. Power Sources* 477 (2020), 228990, <https://doi.org/10.1016/j.jpowsour.2020.228990>.
- [29] A. Krige, U. Rova, P. Christakopoulos, 3D bioprinting on cathodes in microbial electrosynthesis for increased acetate production rate using *Sporomusa ovata*, *J. Environ. Chem. Eng.* 9 (2021), 106189, <https://doi.org/10.1016/j.jece.2021.106189>.
- [30] Y.E. Song, A. Mohamed, C. Kim, M. Kim, S. Li, E. Sundstrom, H. Beyenal, J. R. Kim, Biofilm matrix and artificial mediator for efficient electron transport in CO₂ microbial electrosynthesis, *Chem. Eng. J.* 427 (2022), 131885, <https://doi.org/10.1016/j.cej.2021.131885>.
- [31] X. Xue, Z. Liu, W. Cai, K. Cui, K. Guo, Porous polyurethane particles enhanced the acetate production of a hydrogen-mediated microbial electrosynthesis reactor, *Bioresour. Technol. Rep.* 18 (2022), 101073, <https://doi.org/10.1016/j.biteb.2022.101073>.
- [32] R. Yadav, P. Chiranjeevi, S. Yadav, R. Singh, S.A. Patil, Electricity-driven bioproduction from CO₂ and N₂ feedstocks using enriched mixed microbial culture, *J. CO₂ Util.* 60 (2022), 101997, <https://doi.org/10.1016/j.jcou.2022.101997>.
- [33] H.Y. Yang, N.N. Hou, Y.X. Wang, J. Liu, C.S. He, Y.R. Wang, W.H. Li, Y. Mu, Mixed-culture biocathodes for acetate production from CO₂ reduction in the microbial electrosynthesis: Impact of temperature, *Sci. Total Environ.* 790 (2021), 148128, <https://doi.org/10.1016/j.scitotenv.2021.148128>.
- [34] Q. Fu, Y. He, Z. Li, J. Li, L. Zhang, X. Zhu, Q. Liao, Direct CO₂ delivery with hollow stainless steel/graphene foam electrode for enhanced methane production in microbial electrosynthesis, *Energy Convers. Manag.* 268 (2022), 116018, <https://doi.org/10.1016/j.enconman.2022.116018>.
- [35] R. Nitisoravut, R. Regmi, Plant microbial fuel cells: a promising biosystems engineering, *Renew. Sustain. Energy Rev.* 76 (2017) 81–89, <https://doi.org/10.1016/j.rser.2017.03.064>.
- [36] N. Tongphanpharn, C.-H. Chou, C.-Y. Guan, C.-P. Yu, Plant microbial fuel cells with *Oryza rufipogon* and *Typha orientalis* for remediation of cadmium contaminated soil, *Environ. Technol. Innov.* 24 (2021), 102030, <https://doi.org/10.1016/j.eti.2021.102030>.
- [37] C.-Y. Guan, C.-P. Yu, Evaluation of plant microbial fuel cells for urban green roofs in a subtropical metropolis, *Sci. Total Environ.* 765 (2021), 142786, <https://doi.org/10.1016/j.scitotenv.2020.142786>.
- [38] S. Maddalwar, K. Kumar Nayak, M. Kumar, L. Singh, Plant microbial fuel cell: opportunities, challenges, and prospects, *Bioresour. Technol.* 341 (2021), 125772, <https://doi.org/10.1016/j.biortech.2021.125772>.
- [39] P. Narayana Prasad, S. Kalla, Plant-microbial fuel cells - a bibliometric analysis, *Process Biochem* 111 (2021) 250–260, <https://doi.org/10.1016/j.procbio.2021.10.001>.
- [40] S. Venkata Mohan, G. Mohanakrishna, P. Chiranjeevi, Sustainable power generation from floating macrophytes based ecological microenvironment through embedded fuel cells along with simultaneous wastewater treatment, *Bioresour. Technol.* 102 (2011) 7036–7042, <https://doi.org/10.1016/j.biortech.2011.04.033>.
- [41] H. Wen, H. Zhu, B. Yan, B. Shutes, X. Yu, R. Cheng, X. Chen, X. Wang, Constructed wetlands integrated with microbial fuel cells for COD and nitrogen removal affected by plant and circuit operation mode, *Environ. Sci. Pollut. Res.* 28 (2021) 3008–3018, <https://doi.org/10.1007/s11356-020-10632-3>.
- [42] J.-Y. Xu, H. Xu, X.-L. Yang, R.P. Singh, T. Li, Y. Wu, H.-L. Song, Simultaneous bioelectricity generation and pollutants removal of sediment microbial fuel cell combined with submerged macrophyte, *Int. J. Hydrog. Energy* 46 (2021) 11378–11388, <https://doi.org/10.1016/j.ijhydene.2020.06.007>.
- [43] Z.S. Aswad, A.H. Ali, N.M. Al-Mhanna, Energy production and wastewater treatment using *juncus*, *S. Triquetra*, *P. Australis*, *T. Latifolia*, and *C. Alternifolius* plants in sediment microbial fuel cell, *Desalin. Water Treat.* 205 (2020) 153–160, <https://doi.org/10.5004/dwt.2020.26338>.
- [44] H.Z. Hamdan, A.F. Houry, CO₂ sequestration by propagation of the fast-growing *Azolla* spp, *Environ. Sci. Pollut. Res.* 29 (2022) 16912–16924, <https://doi.org/10.1007/s11356-021-16986-6>.

- [45] R. Regmi, R. Nitisoravut, Azolla enhances electricity generation of paddy microbial fuel cell, *Asean Eng. J.* 10 (2020) 55–63, <https://doi.org/10.11113/aej.v10.15539>.
- [46] F.T. Kabutey, Q. Zhao, L. Wei, J. Ding, P. Antwi, F.K. Quashie, W. Wang, An overview of plant microbial fuel cells (PMFCs): configurations and applications, *Renew. Sustain. Energy Rev.* 110 (2019) 402–414, <https://doi.org/10.1016/j.rser.2019.05.016>.
- [47] Z. Lu, D. Yin, P. Chen, H. Wang, Y. Yang, G. Huang, L. Cai, L. Zhang, Power-generating trees: direct bioelectricity production from plants with microbial fuel cells, *Appl. Energy* 268 (2020), 115040, <https://doi.org/10.1016/j.apenergy.2020.115040>.
- [48] M. Gulamhussein, D.G. Randall, Design and operation of plant microbial fuel cells using municipal sludge, *J. Water Process Eng.* 38 (2020), 101653, <https://doi.org/10.1016/j.jwpe.2020.101653>.
- [49] S.R.B. Arulmani, H.L. Gnanamuthu, S. Kandasamy, G. Govindarajan, M. Alsehl, A. Elfasakhany, A. Pugazhendhi, H. Zhang, Sustainable bioelectricity production from *Amaranthus viridis* and *Triticum aestivum* mediated plant microbial fuel cells with efficient electrogenic bacteria selections, *Process Biochem.* 107 (2021) 27–37, <https://doi.org/10.1016/j.procbio.2021.04.015>.
- [50] T. Saeed, N. Majed, A. Kumar Yadav, A. Hasan, M. Jihad Miah, Constructed wetlands for drained wastewater treatment and sludge stabilization: role of plants, microbial fuel cell and earthworm assistance, *Chem. Eng. J.* 430 (2022), 132907, <https://doi.org/10.1016/j.cej.2021.132907>.
- [51] Y. Xu, Y. Lu, X. Zhu, Toward plant energy harvesting for 5G signal amplification, *ACS Sustain. Chem. Eng.* 9 (2021) 1099–1104, <https://doi.org/10.1021/acssuschemeng.0c08453>.
- [52] E. Osorio-de-la-Rosa, J. Vazquez-Castillo, A. Castillo-Atoche, J. Heredia-Lozano, A. Castillo-Atoche, G. Becerra-Nunez, R. Barbosa, Arrays of plant microbial fuel cells for implementing self-sustainable wireless sensor networks, *IEEE Sens. J.* 21 (2021) 1965–1974, <https://doi.org/10.1109/JSEN.2020.3019986>.
- [53] D. Brunelli, P. Tosato, M. Rossi, Flora health wireless monitoring with plant-microbial fuel cell, *Procedia Eng.* 168 (2016) 1646–1650, <https://doi.org/10.1016/j.proeng.2016.11.481>.
- [54] K. Kumar, S.P. Manangath, P. Manju, S. Gajalakshmi, Resource recovery from paddy field using plant microbial fuel cell, *Process Biochem.* 99 (2020) 270–281, <https://doi.org/10.1016/j.procbio.2020.09.015>.
- [55] J. Md Khudzari, Y. Gariépy, J. Kurian, B. Tartakovsky, G.S.V. Raghavan, Effects of biochar anodes in rice plant microbial fuel cells on the production of bioelectricity, biomass, and methane, *Biochem. Eng. J.* 141 (2019) 190–199, <https://doi.org/10.1016/j.bej.2018.10.012>.
- [56] R.A. Timmers, D.P. Strik, H.V. Hamelers, C.J. Buisman, Electricity generation by a novel design tubular plant microbial fuel cell, *Bioenergy* 51 (2013) 60–67, <https://doi.org/10.1016/j.biombioe.2013.01.002>.
- [57] P.J. Sarma, K. Mohanty, *Epipremnum aureum* and *Dracaena braunii* as indoor plants for enhanced bio-electricity generation in a plant microbial fuel cell with electrochemically modified carbon fiber brush anode, *J. Biosci. Bioeng.* 126 (2018) 404–410, <https://doi.org/10.1016/j.jbiosc.2018.03.009>.
- [58] S. Liu, F. Lu, D. Qiu, X. Feng, Wetland plants selection and electrode optimization for constructed wetland-microbial fuel cell treatment of Cr(VI)-containing wastewater, *J. Water Process Eng.* 49 (2022), 103040, <https://doi.org/10.1016/j.jwpe.2022.103040>.
- [59] R. Piyaare, A.L. Murphy, P. Tosato, D. Brunelli, Plug into a plant: using a plant microbial fuel cell and a wake-up radio for an energy neutral sensing system. 2017 IEEE 42nd Conf. Local Comput. Networks Work. (LCN Work, IEEE, 2017, pp. 18–25, <https://doi.org/10.1109/LCN.Workshops.2017.60>.
- [60] N. Tapia, C. Rojas, C. Bonilla, I. Vargas, A new method for sensing soil water content in green roofs using plant microbial fuel cells, *Sensors* 18 (2017) 71, <https://doi.org/10.3390/s18010071>.
- [61] K.K. Jaiswal, V. Kumar, M.S. Vlaskin, N. Sharma, I. Rautela, M. Nanda, N. Arora, A. Singh, P.K. Chauhan, Microalgae fuel cell for wastewater treatment: recent advances and challenges, *J. Water Process Eng.* 38 (2020), 101549, <https://doi.org/10.1016/j.jwpe.2020.101549>.
- [62] S. Pandit, B.K. Nayak, D. Das, Microbial carbon capture cell using cyanobacteria for simultaneous power generation, carbon dioxide sequestration and wastewater treatment, *Bioresour. Technol.* 107 (2012) 97–102, <https://doi.org/10.1016/j.biortech.2011.12.067>.
- [63] M.M. Ghangrekar, S. Kumar, A. Ahmad, S. Das, Concomitant bioenergy production and wastewater treatment employing microbial electrochemical technologies, *Biofuels Bioenergy* (2022) 359–385, <https://doi.org/10.1016/B978-0-323-85269-2.00015-0>.
- [64] D.A. Jadhav, B. Neethu, M.M. Ghangrekar, Microbial Carbon Capture Cell: Advanced Bio-electrochemical System for Wastewater Treatment, Electricity Generation and Algal Biomass Production, in: *Applied Microalgae Wastewater Treatment*, Springer International Publishing, Cham, 2019, pp. 317–338, https://doi.org/10.1007/978-3-030-13909-4_14.
- [65] D.A. Jadhav, S.C. Jain, M.M. Ghangrekar, Simultaneous wastewater treatment, algal biomass production and electricity generation in clayware microbial carbon capture cells, *Appl. Biochem. Biotechnol.* 183 (2017) 1076–1092, <https://doi.org/10.1007/s12010-017-2485-5>.
- [66] B. Saba, A.D. Christy, Z. Yu, A.C. Co, Sustainable power generation from bacterio-algal microbial fuel cells (MFCs): an overview, *Renew. Sustain. Energy Rev.* 73 (2017) 75–84, <https://doi.org/10.1016/j.rser.2017.01.115>.
- [67] J. Barrett, P. Girr, L.C.M. Mackinder, Pyrenoids: CO₂-fixing phase separated liquid organelles, *Biochim. Biophys. Acta - Mol. Cell Res.* 1868 (2021), 118949, <https://doi.org/10.1016/j.bbamer.2021.118949>.
- [68] H.-W. Yen, S.-H. Ho, C.-Y. Chen, J.-S. Chang, CO₂, NO_x and SO_x removal from flue gas via microalgae cultivation: a critical review, *Biotechnol. J.* 10 (2015) 829–839, <https://doi.org/10.1002/biot.201400707>.
- [69] N. Kannan, P. Donnellan, Algae-assisted microbial fuel cells: a practical overview, *Bioresour. Technol. Rep.* 15 (2021), 100747, <https://doi.org/10.1016/j.biteb.2021.100747>.
- [70] S. Mehrotra, V. Kiran Kumar, K. Man mohan, S. Gajalakshmi, B. Pathak, Bioelectrogenesis from ceramic membrane-based algal-microbial fuel cells treating dairy industry wastewater, *Sustain. Energy Technol. Assess.* 48 (2021), 101653, <https://doi.org/10.1016/j.seta.2021.101653>.
- [71] J.K.N. Amit, U.K. Ghosh, Microalgal remediation of anaerobic pretreated pharmaceutical wastewater for sustainable biodiesel production and electricity generation, *J. Water Process Eng.* 35 (2020), 101192, <https://doi.org/10.1016/j.jwpe.2020.101192>.
- [72] C.D.Y. Yahampath Arachchige Don, S. Babel, Circulation of anodic effluent to the cathode chamber for subsequent treatment of wastewater in photosynthetic microbial fuel cell with generation of bioelectricity and algal biomass, *Chemosphere* 278 (2021), 130455, <https://doi.org/10.1016/j.chemosphere.2021.130455>.
- [73] A. Sharma, S. Gajbihiye, S. Chauhan, M. Chhabra, Effect of cathodic culture on wastewater treatment and power generation in a photosynthetic sediment microbial fuel cell (SMFC): *Canna indica* v/s *Chlorella vulgaris*, *Bioresour. Technol.* 340 (2021), 125645, <https://doi.org/10.1016/j.biortech.2021.125645>.
- [74] M. Oliot, L. Etcheverry, R. Mosdale, A. Bergel, Microbial fuel cells connected in series in a common electrolyte underperform: understanding why and in what context such a set-up can be applied, *Electrochim. Acta* 246 (2017) 879–889, <https://doi.org/10.1016/j.electacta.2017.06.114>.
- [75] S. Naina Mohamed, P. Ajit Hiranman, K. Muthukumar, T. Jayabalan, Bioelectricity production from kitchen wastewater using microbial fuel cell with photosynthetic algal cathode, *Bioresour. Technol.* 295 (2020), 122226, <https://doi.org/10.1016/j.biortech.2019.122226>.
- [76] A. Khandelwal, K. Dhindhoria, A. Dixit, M. Chhabra, Superiority of activated graphite/CuO composite electrode over Platinum based electrodes as cathode in algae assisted microbial fuel cell, *Environ. Technol. Innov.* 24 (2021), 101891, <https://doi.org/10.1016/j.eti.2021.101891>.
- [77] S. Gupta, A. Nayak, C. Roy, A.K. Yadav, An algal assisted constructed wetland-microbial fuel cell integrated with sand filter for efficient wastewater treatment and electricity production, *Chemosphere* 263 (2021), 128132, <https://doi.org/10.1016/j.chemosphere.2020.128132>.
- [78] Z. Yang, H. Pei, Q. Hou, L. Jiang, L. Zhang, C. Nie, Algal biofilm-assisted microbial fuel cell to enhance domestic wastewater treatment: nutrient, organics removal and bioenergy production, *Chem. Eng. J.* 332 (2018) 277–285, <https://doi.org/10.1016/j.cej.2017.09.096>.
- [79] D.A. Jadhav, S.C. Jain, M.M. Ghangrekar, Simultaneous wastewater treatment, algal biomass production and electricity generation in clayware microbial carbon capture cells, *Appl. Biochem. Biotechnol.* 183 (2017) 1076–1092, <https://doi.org/10.1007/s12010-017-2485-5>.
- [80] Z. Yang, L. Zhang, C. Nie, Q. Hou, S. Zhang, H. Pei, Multiple anodic chambers sharing an algal raceway pond to establish a photosynthetic microbial fuel cell stack: voltage boosting accompany wastewater treatment, *Water Res.* 164 (2019), 114955, <https://doi.org/10.1016/j.watres.2019.114955>.
- [81] S. Das, S. Das, M.M. Ghangrekar, Quorum-sensing mediated signals: a promising multi-functional modulators for separately enhancing algal yield and power generation in microbial fuel cell, *Bioresour. Technol.* 294 (2019), 122138, <https://doi.org/10.1016/j.biortech.2019.122138>.
- [82] S. Liu, R. Wang, C. Ma, D. Yang, D. Li, Z. Lewandowski, Improvement of electrochemical performance via enhanced reactive oxygen species adsorption at ZnO–NiO-rGO carbon felt cathodes in photosynthetic algal microbial fuel cells, *Chem. Eng. J.* 391 (2020), 123627, <https://doi.org/10.1016/j.cej.2019.123627>.
- [83] C.D.Y. Yahampath Arachchige Don, S. Babel, Effects of ammonium concentration in the catholyte on electricity and algal biomass generation in a photosynthetic microbial fuel cell treating wastewater, *Bioresour. Technol. Rep.* 16 (2021), 100867, <https://doi.org/10.1016/j.biteb.2021.100867>.
- [84] Y. Zhang, L. Gong, Q. Jiang, M.-H. Cui, J. Zhang, H. Liu, In-situ CO₂ sequestration and nutrients removal in an anaerobic digestion-microbial electrolysis cell by silicates application: Effect of dosage and biogas circulation, *Chem. Eng. J.* 399 (2020), 125680, <https://doi.org/10.1016/j.cej.2020.125680>.
- [85] X. Zhu, C. Lei, J. Qi, G. Zhen, X. Lu, S. Xu, J. Zhang, H. Liu, X. Zhang, Z. Wu, The role of microbiome in carbon sequestration and environment security during wastewater treatment, *Sci. Total Environ.* 837 (2022), 155793, <https://doi.org/10.1016/j.scitotenv.2022.155793>.
- [86] Y. Zhang, Q. Jiang, L. Gong, H. Liu, M. Cui, J. Zhang, In-situ mineral CO₂ sequestration in a methane producing microbial electrolysis cell treating sludge hydrolysate, *J. Hazard. Mater.* 394 (2020), 122519, <https://doi.org/10.1016/j.jhazmat.2020.122519>.
- [87] M. Cui, H. Nie, T. Zhang, D. Lovley, T.P. Russell, Three-dimensional hierarchical metal oxide-carbon electrode materials for highly efficient microbial electrosynthesis, *Sustain. Energy Fuels* 1 (2017) 1171–1176, <https://doi.org/10.1039/c7se00073a>.
- [88] T. Zhang, H. Nie, T.S. Bain, H. Lu, M. Cui, O.L. Snoeyenbos-West, A.E. Franks, K. P. Nevin, T.P. Russell, D.R. Lovley, Improved cathode materials for microbial electrosynthesis, *Energy Environ. Sci.* 6 (2013) 217–224, <https://doi.org/10.1039/c2ee23350a>.
- [89] H. Nie, T. Zhang, M. Cui, H. Lu, D.R. Lovley, T.P. Russell, Improved cathode for high efficient microbial-catalyzed reduction in microbial electrosynthesis cells,

- Phys. Chem. Chem. Phys. 15 (2013) 14290–14294, <https://doi.org/10.1039/c3cp52697f>.
- [90] L. Jourdain, S. Freguía, B.C. Donose, J. Chen, G.G. Wallace, J. Keller, V. Flexer, A novel carbon nanotube modified scaffold as an efficient biocathode material for improved microbial electrosynthesis, *J. Mater. Chem. A*. 2 (2014) 13093–13102, <https://doi.org/10.1039/c4ta03101f>.
 - [91] Z. Dong, H. Wang, S. Tian, Y. Yang, H. Yuan, Q. Huang, T. Song, J. Xie, Fluidized granular activated carbon electrode for efficient microbial electrosynthesis of acetate from carbon dioxide, *Bioresour. Technol.* 269 (2018) 203–209, <https://doi.org/10.1016/j.biortech.2018.08.103>.
 - [92] X. Li, J. Wen, J. Low, Y. Fang, J. Yu, Design and fabrication of semiconductor photocatalyst for photocatalytic reduction of CO₂ to solar fuel, *Sci. China Mater.* 57 (2014) 70–100, <https://doi.org/10.1007/s40843-014-0003-1>.
 - [93] M. Priyadarshini, I. Das, M.M. Ghangrekar, L. Blaney, Advanced oxidation processes: performance, advantages, and scale-up of emerging technologies, *J. Environ. Manag.* 316 (2022), 115295, <https://doi.org/10.1016/j.jenvman.2022.115295>.
 - [94] J. Wu, Y. Huang, W. Ye, Y. Li, CO₂ reduction: from the electrochemical to photochemical approach, *Adv. Sci.* 4 (2017), 1700194, <https://doi.org/10.1002/advs.201700194>.
 - [95] X. Chen, S.S. Mao, Titanium dioxide nanomaterials: synthesis, properties, modifications and applications, *Chem. Rev.* 107 (2007) 2891–2959, <https://doi.org/10.1021/cr0500535>.
 - [96] S. Nahar, M.F.M. Zain, A.A.H. Kadhum, H.A. Hasan, M.R. Hasan, Advances in photocatalytic CO₂ reduction with water: a review, *Materials* 10 (2017), <https://doi.org/10.3390/ma10060629>.
 - [97] J. Low, B. Cheng, J. Yu, Surface modification and enhanced photocatalytic CO₂ reduction performance of TiO₂: a review, *Appl. Surf. Sci.* 392 (2017) 658–686, <https://doi.org/10.1016/j.apsusc.2016.09.093>.
 - [98] Q. Huang, J. Yu, S. Cao, C. Cui, B. Cheng, Efficient photocatalytic reduction of CO₂ by amine-functionalized g-C₃N₄, *Appl. Surf. Sci.* (2015) 350–355, <https://doi.org/10.1016/j.apsusc.2015.07.082>.
 - [99] X. Chen, S. Shen, L. Guo, S.S. Mao, Semiconductor-based photocatalytic hydrogen generation, *Chem. Rev.* 110 (2010) 6503–6570, <https://doi.org/10.1021/cr1001645>.
 - [100] A. Kudo, Y. Miseki, Heterogeneous photocatalyst materials for water splitting, *Chem. Soc. Rev.* 38 (2009) 253–278, <https://doi.org/10.1039/b800489g>.
 - [101] Y. Inoue, Photocatalytic water splitting by RuO₂-loaded metal oxides and nitrides with d0- and d10 -related electronic configurations, *Energy Environ. Sci.* 2 (2009) 364–386, <https://doi.org/10.1039/b816677n>.
 - [102] Y. Sohn, W. Huang, F. Taghipour, Recent progress and perspectives in the photocatalytic CO₂ reduction of Ti-oxide-based nanomaterials, *Appl. Surf. Sci.* 396 (2017) 1696–1711, <https://doi.org/10.1016/j.apsusc.2016.11.240>.
 - [103] K. Li, B. Peng, T. Peng, Recent advances in heterogeneous photocatalytic CO₂ conversion to solar fuels, *ACS Catal.* 6 (2016) 7485–7527, <https://doi.org/10.1021/acscatal.6b02089>.
 - [104] V.P. Indrakanti, J.D. Kubicki, H.H. Schobert, Quantum chemical modeling of ground states of CO₂ chemisorbed on anatase (001), (101), and (010) TiO₂ surfaces, *Energy Fuels* 22 (2008) 2611–2618, <https://doi.org/10.1021/ef700725u>.
 - [105] M.M. Rodriguez, X. Peng, L. Liu, Y. Li, J.M. Andino, A density functional theory and experimental study of CO₂ interaction with brookite TiO₂, *J. Phys. Chem. C*. 116 (2012) 19755–19764, <https://doi.org/10.1021/jp302342t>.
 - [106] X. Chen, Y. Zhou, Q. Liu, Z. Li, J. Liu, Z. Zou, Ultrathin, single-crystal WO₃ nanosheets by two-dimensional oriented attachment toward enhanced photocatalytic reduction of CO₂ into hydrocarbon fuels under visible light, *ACS Appl. Mater. Interfaces* 4 (2012) 3372–3377, <https://doi.org/10.1021/am300661s>.
 - [107] S. Feng, X. Chen, Y. Zhou, W. Tu, P. Li, H. Li, Z. Zou, Na₂V₆O₁₆·xH₂O nanoribbons: Large-scale synthesis and visible-light photocatalytic activity of CO₂ into solar fuels, *Nanoscale* 6 (2014) 1896–1900, <https://doi.org/10.1039/c3nr05219b>.
 - [108] Q. Liu, Y. Zhou, J. Kou, X. Chen, Z. Tian, J. Gao, S. Yan, Z. Zou, High-yield synthesis of ultralong and ultrathin Zn₂GeO₄ nanoribbons toward improved photocatalytic reduction of CO₂ into renewable hydrocarbon fuel, *J. Am. Chem. Soc.* 132 (2010) 14385–14387, <https://doi.org/10.1021/ja1068596>.
 - [109] S.C. Yan, S.X. Ouyang, J. Gao, M. Yang, J.Y. Feng, X.X. Fan, L.J. Wan, Z.S. Li, J. H. Ye, Y. Zhou, Z.G. Zou, A room-temperature reactive-template route to mesoporous ZnGa₂O₄ with improved photocatalytic activity in reduction of CO₂, *Angew. Chem.* 122 (2010) 6544–6548, <https://doi.org/10.1002/ange.201003270>.
 - [110] B.R. Egnins, J.T.S. Irvine, E.P. Murphy, J. Grimshaw, Formation of two-carbon acids from carbon dioxide by photoreduction on cadmium sulphide, *J. Chem. Soc. Chem. Trans.* (1988) 1123–1124, <https://doi.org/10.1039/C39880001123>.
 - [111] S. Wang, X. Wang, Photocatalytic CO₂ reduction by CdS promoted with a zeolitic imidazolate framework, *Appl. Catal. B Environ.* 162 (2015) 494–500, <https://doi.org/10.1016/j.apcatb.2014.07.026>.
 - [112] T. Baran, S. Wojtyła, A. Dibeneditto, M. Aresta, W. Macyk, Zinc sulfide functionalized with ruthenium nanoparticles for photocatalytic reduction of CO₂, *Appl. Catal. B Environ.* 178 (2015) 170–176, <https://doi.org/10.1016/j.apcatb.2014.09.052>.
 - [113] T. Baran, A. Dibeneditto, M. Aresta, K. Kruczała, W. Macyk, Photocatalytic carboxylation of organic substrates with carbon dioxide at zinc sulfide with deposited ruthenium nanoparticles, *Chempluschem* 79 (2014) 708–715, <https://doi.org/10.1002/cplu.201300438>.
 - [114] Y. Li, W.N. Wang, Z. Zhan, M.H. Woo, C.Y. Wu, P. Biswas, Photocatalytic reduction of CO₂ with H₂O on mesoporous silica supported Cu/TiO₂ catalysts, *Appl. Catal. B Environ.* 100 (2010) 386–392, <https://doi.org/10.1016/j.apcatb.2010.08.015>.
 - [115] H.C. Hsu, I. Shown, H.Y. Wei, Y.C. Chang, H.Y. Du, Y.G. Lin, C.A. Tseng, C. H. Wang, L.C. Chen, Y.C. Lin, K.H. Chen, Graphene oxide as a promising photocatalyst for CO₂ to methanol conversion, *Nanoscale* 5 (2013) 262–268, <https://doi.org/10.1039/c2nr31718d>.
 - [116] W.J. Ong, M.M. Gui, S.P. Chai, A.R. Mohamed, Direct growth of carbon nanotubes on Ni/TiO₂ as next generation catalysts for photoreduction of CO₂ to methane by water under visible light irradiation, *RSC Adv.* 3 (2013) 4505–4509, <https://doi.org/10.1039/c3ra00030c>.
 - [117] M. Tahir, N.A.S. Amin, Photocatalytic reduction of carbon dioxide with water vapors over montmorillonite modified TiO₂ nanocomposites, *Appl. Catal. B Environ.* 142–143 (2013) 512–522, <https://doi.org/10.1016/j.apcatb.2013.05.054>.
 - [118] Y. He, L. Zhang, M. Fan, X. Wang, M.L. Walbridge, Q. Nong, Y. Wu, L. Zhao, Z-scheme SnO₂-x/g-C₃N₄ composite as an efficient photocatalyst for dye degradation and photocatalytic CO₂ reduction, *Sol. Energy Mater. Sol. Cells* 137 (2015) 175–184, <https://doi.org/10.1016/j.solmat.2015.01.037>.
 - [119] W. Tu, Y. Zhou, Q. Liu, Z. Tian, J. Gao, X. Chen, H. Zhang, J. Liu, Z. Zou, Robust hollow spheres consisting of alternating titania nanosheets and graphene nanosheets with high photocatalytic activity for CO₂ conversion into renewable fuels, *Adv. Funct. Mater.* 22 (2012) 1215–1221, <https://doi.org/10.1002/adfm.201102566>.
 - [120] L. Liang, F. Lei, S. Gao, Y. Sun, X. Jiao, J. Wu, S. Qamar, Y. Xie, Single unit cell bismuth tungstate layers realizing robust solar CO₂ reduction to methanol, *Angew. Chem.* 127 (2015) 14177–14180, <https://doi.org/10.1002/ange.201506966>.
 - [121] P. Li, Y. Zhou, Z. Zhao, Q. Xu, X. Wang, M. Xiao, Z. Zou, Hexahedron prism-anchored octahedral CeO₂: crystal facet-based homojunction promoting efficient solar fuel synthesis, *J. Am. Chem. Soc.* 137 (2015) 9547–9550, <https://doi.org/10.1021/jacs.5b05926>.
 - [122] A. Manzi, T. Simon, C. Sonnleitner, M. Döblinger, R. Wyrwich, O. Stern, J. K. Stolarczyk, J. Feldmann, Light-induced cation exchange for copper sulfide based CO₂ reduction, *J. Am. Chem. Soc.* 137 (2015) 14007–14010, <https://doi.org/10.1021/jacs.5b06778>.
 - [123] N. Sun, M. Zhou, X. Ma, Z. Cheng, J. Wu, Y. Qi, Y. Sun, F. Zhou, Y. Shen, S. Lu, Self-assembled spherical In₂O₃/BiOI heterojunctions for enhanced photocatalytic CO₂ reduction activity, *J. CO₂ Util.* 65 (2022), 102220, <https://doi.org/10.1016/j.jcou.2022.102220>.
 - [124] J. Chen, S. Qin, G. Song, T. Xiang, F. Xin, X. Yin, Shape-controlled solvothermal synthesis of Bi₂S₃ for photocatalytic reduction of CO₂ to methyl formate in methanol, *Dalt. Trans.* 42 (2013) 15133–15138, <https://doi.org/10.1039/c3dt51887f>.
 - [125] D. Wang, R. Huang, W. Liu, D. Sun, Z. Li, Fe-based MOFs for photocatalytic CO₂ reduction: Role of coordination unsaturated sites and dual excitation pathways, *ACS Catal.* 4 (2014) 4254–4260, <https://doi.org/10.1021/cs501169t>.
 - [126] D. Sun, Y. Fu, W. Liu, L. Ye, D. Wang, L. Yang, X. Fu, Z. Li, Studies on photocatalytic CO₂ reduction over NH₂-uio-66(Zr) and its derivatives: Towards a better understanding of photocatalysis on metal-organic frameworks, *Chem. - A Eur. J.* 19 (2013) 14279–14285, <https://doi.org/10.1002/chem.201301728>.
 - [127] M. Priyadarshini, A. Ahmad, S. Das, M.M. Ghangrekar, Metal organic frameworks as emergent oxygen-reducing cathode catalysts for microbial fuel cells: a review, *Int. J. Environ. Sci. Technol.* (2021), <https://doi.org/10.1007/s13762-021-03499-5>.
 - [128] M. Priyadarshini, I. Das, M.M. Ghangrekar, Application of metal organic framework in wastewater treatment and detection of pollutants: review, *J. Indian Chem. Soc.* 97 (2020) 507–512.
 - [129] Y. Fu, D. Sun, Y. Chen, R. Huang, Z. Ding, X. Fu, Z. Li, An amine-functionalized titanium metal-organic framework photocatalyst with visible-light-induced activity for CO₂ reduction, *Angew. Chem. - Int. Ed.* 51 (2012) 3364–3367, <https://doi.org/10.1002/anie.201108357>.
 - [130] M.W. Logan, S. Ayad, J.D. Adamson, T. Dilbeck, K. Hanson, F.J. Uribe-Romo, Systematic variation of the optical bandgap in titanium based isorecticular metal-organic frameworks for photocatalytic reduction of CO₂ under blue light, *J. Mater. Chem. A*. 5 (2017) 11854–11863, <https://doi.org/10.1039/c7ta00437k>.
 - [131] A. Ahmad, M. Priyadarshini, S. Yadav, M.M. Ghangrekar, R.Y. Surampalli, The potential of biochar-based catalysts in advanced treatment technologies for efficacious removal of persistent organic pollutants from wastewater: a review, *Chem. Eng. Res. Des.* 187 (2022) 470–496, <https://doi.org/10.1016/j.cherd.2022.09.024>.
 - [132] X.L. Luo, Z. Yin, M.H. Zeng, M. Kurmoo, The construction, structures, and functions of pillared layer metal-organic frameworks, *Inorg. Chem. Front.* 3 (2016) 1208–1226, <https://doi.org/10.1039/c6qi00181e>.
 - [133] J. Mao, T. Peng, X. Zhang, K. Li, L. Ye, L. Zan, Effect of graphitic carbon nitride microstructures on the activity and selectivity of photocatalytic CO₂ reduction under visible light, *Catal. Sci. Technol.* 3 (2013) 1253–1260, <https://doi.org/10.1039/c3cy20822b>.
 - [134] R. Kuriki, K. Sekizawa, O. Ishitani, K. Maeda, Visible-light-driven CO₂ reduction with carbon nitride: Enhancing the activity of ruthenium catalysts, *Angew. Chem. - Int. Ed.* 54 (2015) 2406–2409, <https://doi.org/10.1002/anie.201411170>.
 - [135] L. Shi, T. Wang, H. Zhang, K. Chang, J. Ye, Electrostatic self-assembly of nanosized carbon nitride nanosheet onto a zirconium metal-organic framework for enhanced photocatalytic CO₂ reduction, *Adv. Funct. Mater.* 25 (2015) 5360–5367, <https://doi.org/10.1002/adfm.201502253>.

- [136] A. Ahmad, M. Priyadarshini, S. Das, M.M. Ghangrekar, Proclaiming electrochemical oxidation as a potent technology for the treatment of wastewater containing xenobiotic compounds: a mini review, *J. Hazard., Toxic., Radioact. Waste* 25 (2021) 1–13, [https://doi.org/10.1061/\(asce\)hz.2153-5515.0000616](https://doi.org/10.1061/(asce)hz.2153-5515.0000616).
- [137] M. Priyadarshini, A. Ahmad, S. Das, M.M. Ghangrekar, Application of innovative electrochemical and microbial electrochemical technologies for the efficacious removal of emerging contaminants from wastewater: a review, *J. Environ. Chem. Eng.* 10 (2022), 108230, <https://doi.org/10.1016/j.jece.2022.108230>.
- [138] E.E. Benson, C.P. Kubiak, A.J. Sathrum, J.M. Smieja, Electrocatalytic and homogeneous approaches to conversion of CO₂ to liquid fuels, *Chem. Soc. Rev.* 38 (2009) 89–99, <https://doi.org/10.1039/b804323j>.
- [139] W. Leitner, Carbon Dioxide as a Raw Material: The Synthesis of Formic Acid and Its Derivatives from CO₂, 1995, doi: 10.1002/anie.199522071.
- [140] D. Xu, K. Li, B. Jia, W. Sun, W. Zhang, X. Liu, T. Ma, Electrocatalytic CO₂ reduction towards industrial applications, *Carbon Energy* (2022), <https://doi.org/10.1002/cey2.230>.
- [141] A.D.N. Kamkeng, M. Wang, J. Hu, W. Du, F. Qian, Transformation technologies for CO₂ utilisation: Current status, challenges and future prospects, *Chem. Eng. J.* 409 (2021), 128138, <https://doi.org/10.1016/j.cej.2020.128138>.
- [142] W. Ma, S. Xie, T. Liu, Q. Fan, J. Ye, F. Sun, Z. Jiang, Q. Zhang, J. Cheng, Y. Wang, Electrocatalytic reduction of CO₂ to ethylene and ethanol through hydrogen-assisted C–C coupling over fluorine-modified copper, *Nat. Catal.* 3 (2020) 478–487, <https://doi.org/10.1038/s41929-020-0450-0>.
- [143] M. Gattrell, N. Gupta, A. Co, A review of the aqueous electrochemical reduction of CO₂ to hydrocarbons at copper, *J. Electroanal. Chem.* 594 (2006) 1–19, <https://doi.org/10.1016/j.jelechem.2006.05.013>.
- [144] F. Li, D.R. MacFarlane, J. Zhang, Recent advances in the nanoengineering of electrocatalysts for CO₂ reduction, *Nanoscale* 10 (2018) 6235–6260, <https://doi.org/10.1039/c7nr09620h>.
- [145] J.P. Jones, G.K.S. Prakash, G.A. Olah, Electrochemical CO₂ reduction: recent advances and current trends, *Isr. J. Chem.* 54 (2014) 1451–1466, <https://doi.org/10.1002/ijch.201400081>.
- [146] R. Reske, H. Mistry, F. Beharfarid, B. Roldan Cuenya, P. Strasser, Particle size effects in the catalytic electroreduction of CO₂ on Cu nanoparticles, *J. Am. Chem. Soc.* 136 (2014) 6978–6986, <https://doi.org/10.1021/ja500328k>.
- [147] Y. Yoon, A.S. Hall, Y. Surendranath, Tuning of silver catalyst mesostructure promotes selective carbon dioxide conversion into fuels, *Angew. Chem.* 128 (2016) 15508–15512, <https://doi.org/10.1002/ange.201607942>.
- [148] S. Zhang, P. Kang, S. Ubnoske, M.K. Brennaman, N. Song, R.L. House, J.T. Glass, T.J. Meyer, Polyethylenimine-enhanced electrocatalytic reduction of CO₂ to formate at nitrogen-doped carbon nanomaterials, *J. Am. Chem. Soc.* 136 (2014) 7845–7848, <https://doi.org/10.1021/ja5031529>.
- [149] S. Rasul, D.H. Anjum, A. Jedidi, Y. Minenkov, L. Cavallo, K. Takanabe, A highly selective copper-indium bimetallic electrocatalyst for the electrochemical reduction of aqueous CO₂ to CO, *Angew. Chem.* 127 (2015) 2174–2178, <https://doi.org/10.1002/ange.201410233>.
- [150] M. Asadi, K. Kim, C. Liu, A.V. Addepalli, P. Abbasi, P. Yasaei, P. Phillips, A. Behranginia, J.M. Cerrato, R. Haasch, P. Zapol, B. Kumar, R.F. Klie, J. Abiade, L.A. Curtiss, A. Salehi-Khojin, Nanostructured transition metal dichalcogenide electrocatalysts for CO₂ reduction in ionic liquid, *Sci. (80-.)* 353 (2016) 467–470, <https://doi.org/10.1126/science.aaf4767>.
- [151] J. Wu, S. Ma, J. Sun, J.I. Gold, C. Tiwary, B. Kim, L. Zhu, N. Chopra, I.N. Odeh, R. Vajtai, A.Z. Yu, R. Luo, J. Lou, G. Ding, P.J.A. Kenis, P.M. Ajayan, A metal-free electrocatalyst for carbon dioxide reduction to multi-carbon hydrocarbons and oxygenates, *Nat. Commun.* 7 (2016), <https://doi.org/10.1038/ncomms13869>.
- [152] M. Asadi, B. Kumar, A. Behranginia, B.A. Rosen, A. Baskin, N. Repnin, D. Pisasale, P. Phillips, W. Zhu, R. Haasch, R.F. Klie, P. Král, J. Abiade, A. Salehi-Khojin, Robust carbon dioxide reduction on molybdenum disulphide edges, *Nat. Commun.* 5 (2014) 1–8, <https://doi.org/10.1038/ncomms5470>.
- [153] J. Li, Y. Tian, Y. Zhou, Y. Zong, N. Yang, M. Zhang, Z. Guo, Abiotic – biological hybrid systems for - CO₂ conversion to value - added chemicals and fuels, *Trans. Tianjin Univ.* 26 (2020) 237–247, <https://doi.org/10.1007/s12209-020-00257-5>.
- [154] C. Li, K.L. Lesnik, H. Liu, Bioelectrochemistry conductive properties of methanogenic biofilms, *Bioelectrochemistry* 119 (2018) 220–226, <https://doi.org/10.1016/j.bioelechem.2017.10.006>.
- [155] F. Gong, H. Zhu, Y. Zhang, Y. Li, Biological carbon fixation: from natural to synthetic, *J. CO₂ Util.* 28 (2018) 221–227, <https://doi.org/10.1016/j.jcou.2018.09.014>.
- [156] Y. Bai, L. Zhou, M. Irfan, T.T. Liang, L. Cheng, Y.F. Liu, J.F. Liu, S.Z. Yang, W. Sand, J.D. Gu, B.Z. Mu, Bioelectrochemical methane production from CO₂ by *Methanosarcina barkeri* via direct and H₂-mediated indirect electron transfer, *Energy* 210 (2020), 118445, <https://doi.org/10.1016/j.energy.2020.118445>.
- [157] F. Kracke, J.S. Deutzmann, W. Gu, A.M. Spormann, In situ electrochemical H₂ production for efficient and stable power-to-gas electromethanogenesis, *Green. Chem.* 22 (2020) 6194–6203, <https://doi.org/10.1039/d0gc01894e>.
- [158] Q. Fu, S. Xiao, Z. Li, Y. Li, H. Kobayashi, J. Li, Y. Yang, Hybrid solar-to-methane conversion system with a Faradaic efficiency of up, *Nano Energy* 53 (2018) 232–239, <https://doi.org/10.1016/j.nanoen.2018.08.051>.
- [159] J. Ye, G. Ren, L. Kang, Y. Zhang, X. Liu, S. Zhou, Z. He, Efficient photoelectron capture by Ni Decoration in *Methanosarcina barkeri*-CdS biohybrids for enhanced photocatalytic CO₂-to-CH₄ conversion, *IScience* 23 (2020), 101287, <https://doi.org/10.1016/j.isci.2020.101287>.
- [160] J.S. Deutzmann, A.M. Spormann, Enhanced microbial electrosynthesis by using defined co-cultures, *Int. Soc. Microb. Ecol.* 11 (2017) 704–714, <https://doi.org/10.1038/ismej.2016.149>.
- [161] Q. Li, Q. Fu, H. Kobayashi, Y. He, Z. Li, J. Li, GO/PEDOT modified biocathodes promoting CO₂ reduction to CH₄ in microbial electrosynthesis, *Sustain. Energy Fuels* 4 (2020) 2987–2997, <https://doi.org/10.1039/d0se00321b>.
- [162] R.G. Grim, Z. Huang, M.T. Guarnieri, J.R. Ferrell, L. Tao, J.A. Schaidle, Transforming the carbon economy: challenges and opportunities in the convergence of low-cost electricity and reductive CO₂ utilization, *Energy Environ. Sci.* 13 (2020) 472–494, <https://doi.org/10.1039/C9EE02410G>.
- [163] S.M. Jarvis, S. Samsatli, Technologies and infrastructures underpinning future CO₂ value chains: a comprehensive review and comparative analysis, *Renew. Sustain. Energy Rev.* 85 (2018) 46–68, <https://doi.org/10.1016/j.rser.2018.01.007>.
- [164] M. Pérez-Fortes, J.C. Schöneberger, A. Boulamanti, G. Harrison, E. Tzimas, Formic acid synthesis using CO₂ as raw material: techno-economic and environmental evaluation and market potential, *Int. J. Hydrog. Energy* 41 (2016) 16444–16462, <https://doi.org/10.1016/j.ijhydene.2016.05.199>.
- [165] A.S. Agarwal, Y. Zhai, D. Hill, N. Sridhar, The electrochemical reduction of carbon dioxide to formate/formic acid: engineering and economic feasibility, *ChemSusChem* 4 (2011) 1301–1310, <https://doi.org/10.1002/cssc.201100220>.
- [166] F. Madugu, M. Collu, Parametric analysis for an algal oil production process, *Int. J. Energy Prod. Manag* 1 (2016) 141–154, <https://doi.org/10.2495/EQ-V1-N2-141-154>.
- [167] E.M. Trentacoste, A.M. Martinez, T. Zenk, The place of algae in agriculture: policies for algal biomass production, *Photosynth. Res.* 123 (2015) 305–315, <https://doi.org/10.1007/s11120-014-9985-8>.
- [168] O.G. Sánchez, Y.Y. Birdja, M. Bulut, J. Vaes, T. Breugelmans, D. Pant, Recent advances in industrial CO₂ electroreduction, *Curr. Opin. Green. Sustain. Chem.* 16 (2019) 47–56, <https://doi.org/10.1016/j.cogsc.2019.01.005>.